United Nations Educational, Scientific and Cultural Organization
GRÓ GTP Geothermal Training Programme Under the auspices of UNESCO

GRÓ GTP, Grensásvegur 9,
IS-108 Reykjavík, Iceland

Reports 2021
Number 17

EVALUATION OF TRACER TEST RESULTS IN OLKARIA NORTHEAST GEOTHERMAL FIELD, KENYA, AND ITS IMPLICATIONS ON RESOURCE MANAGEMENT

Erique Nyawir
Kenya Electricity Generation Company Limited,
P.O. Box 785-20117,
Naivasha,
KENYA
ENyawir@kengen.co.ke

ABSTRACT

Reservoir management is vital to sustainable geothermal energy production and a robust re-injection strategy is one of the essential reservoir management techniques used in developed geothermal fields. Such a strategy is not only environmentally friendly but also, by maintaining the subsurface pressure, goes a long way in ensuring that the geothermal reservoir is not being depleted. To develop a good re-injection system, it is necessary to understand the geothermal field´s reservoir fluid chemistry and flow patterns to study the connectivity of a reinjection well to other wells nearby. This can be done by undertaking tracer tests. Tracer testing started in the early 90´s in the Olkaria´s East (OEPF) and Northeast (ONEPF) production fields though geothermal utilization has been undertaken in the Greater Olkaria Volcanic Complex for the last 40 years, starting with the commissioning of Olkaria 1 Unit I in June 1981. The latest tracer injection of sodium fluorescein in ONEPF was done in December 2020 into well OW-703. The tracer recovery was thereafter monitored for about six months in most of the production wells in the vicinity. This study evaluates the effects of injection on the production wells in the vicinity by looking at the injection process, production well samples, tracer analysis, and data interpretation. The tracer had a breakthrough in several wells in the field including wells OW-714 (2.0%) and OW-730A (1.2%) implying connections with OW-703. These connections were modelled using the TRINV software which showed that although the re-injected brine has, optimistically, a temperature of 150°C, thermal breakthrough would not be significant in the next 10 years in other wells. However, it was noted that the tracer used, sodium fluorescein, usually decays at high temperatures thus the cooling predictions are likely to be somewhat optimistic. Therefore, it is recommended that tracer testing is repeated using other, more suitable tracers.

1. INTRODUCTION

Energy plays a crucial role in the development of any country. Its effects can be felt in all aspects of human life including food/nutrition, clean water, transport, education, wealth, business, domesticity, and, most importantly, health and life expectancy. Currently over 80% of the primary energy in the

world is derived from non-renewables sources like fossil fuels-oil, coal, natural gas, and nuclear energy (Lloyd, 2017).

Kenya has a total installed electrical generation capacity of 2,945 MW_e out of which 2,191 MW_e is from renewable sources (Table 1). Renewable sources, therefore, account for 74.4% of the total installed electricity generation capacity in the country (IRENA, 2021). Kenya's geothermal capacity is currently 824 MW_e with KenGen's capacity in the Olkaria geothermal field being 703.5 MW_e (85%). The installed geothermal capacity accounts for about 38% of the total renewable energy capacity of the country. KenGen generates geothermal energy from five conventional power plants (Olkaria I, Olkaria IAU, Olkaria II, Olkaria IV and Olkaria V) and several wellhead units spread across its two licenced fields (Olkaria and Eburru).

TABLE 1: Renewable energy sources in Kenya (IRENA, 2021)

Type	Hydro	Geothermal	Wind	Solar	Biomass	**TOTAL**
MW_e	837	824	336	106	88	2,191
%	38.2	37.6	15.3	4.8	4.1	100%

Though installed hydropower capacity in Kenya is the highest of all the renewable energy sources (837 MW_e), its generation is directly influenced by water resources. These resources are affected by climate change-related events which are, thus, significantly influencing the sustainability of hydropower as a reliable source of renewable energy in Kenya (Bunyasi, 2012). Of the annual consumption of electricity from the national grid in Kenya, 47% come from geothermal, 39% from hydropower, 13% from thermal and 0.4 % from wind (Mangi, 2018). In the country´s strategic planning, Kenya´s Least Cost Power Development Plan, geothermal power has been identified as a cost-effective power option (KPLC, 2001). This means that geothermal energy is the leading, reliable, and widely available baseload stable power in Kenya´s national electricity grid.

Geothermal energy, therefore, plays a key role in the sustainable development of Kenya, and thus the country needs to have a robust resource management strategy in place for its use. An important component of such a strategy is the re-injection of spent geothermal fluid back into geothermal systems. The importance of re-injection is two-fold: it assists in maintaining reservoir pressure and increases the energy extraction efficiency over the life of the resource (Kaya et al., 2011; Diaz et al., 2015). To help evaluate the effectiveness of re-injection, tracer testing can be used as tool. Tracer testing assists in characterizing the geothermal system by helping trace the fluid flow paths in the reservoir. Therefore, once tracer testing is done, it is easier to estimate connections between wells and predict thermal breakthrough due to re-injection, and thus mitigate it (Koech, 2014).

The main objective of this study is to look at how re-injection has been managed in Olkaria geothermal field in Kenya with a specific emphasis on the Olkaria Northeast Production Field (ONEPF). This study will also evaluate the effectiveness of hot brine re-injection into well OW-703 and generally the role of tracer testing in resource management. The specific objectives of this study are:

- To evaluate the change in mass flows, well pressures and enthalpies of the wells in the study area, over time.
- To find out if there are any connections between the re-injection well OW-703 and other wells in the vicinity (OEPF and ONEPF).
- To evaluate the possibility of tracer-decay due to high reservoir temperatures in the two sectors.
- To estimate the cooling of connected production wells, due to re-injection of brine into well OW-703.
- The findings of the study will also be used for updating the Olkaria conceptual model.

2. BACKGROUND INFORMATION ON THE STUDY AREA

2.1 Olkaria geothermal system

Olkaria is a high temperature geothermal field and is known for being the oldest and the most explored geothermal field in Kenya (Ouma, 2009). It is located within the Greater Olkaria Volcanic Complex (OVC) and is part of the greater East African Rift System (EARS), a region associated with Quaternary volcanism overlying products of Miocene and Pliocene volcanism (Omenda, 1998). The EARS is divided into two parts: the western and the eastern branch. The Kenyan rift system (KRS), in which Olkaria is located, is part of the eastern branch (Roberts et al., 2012; Baker, 1987). Other volcanic centres in the KRS include Barrier to the north and Lake Magadi in the south (Figure 1). Olkaria is located approximately 120 km NW of Nairobi, on the floor of the southern segment of Kenya's Rift valley. The geothermal field is currently being exploited by two companies: KenGen PLC in the East and Ormat PLC in the West. Olkaria is one of two KenGen fields in Kenya where geothermal energy has been developed for power generation, the other field being Eburru. KenGen has drilled over 300 geothermal wells (both vertical and directional) for production, re-injection, and monitoring within its 204 km^2 concession area.

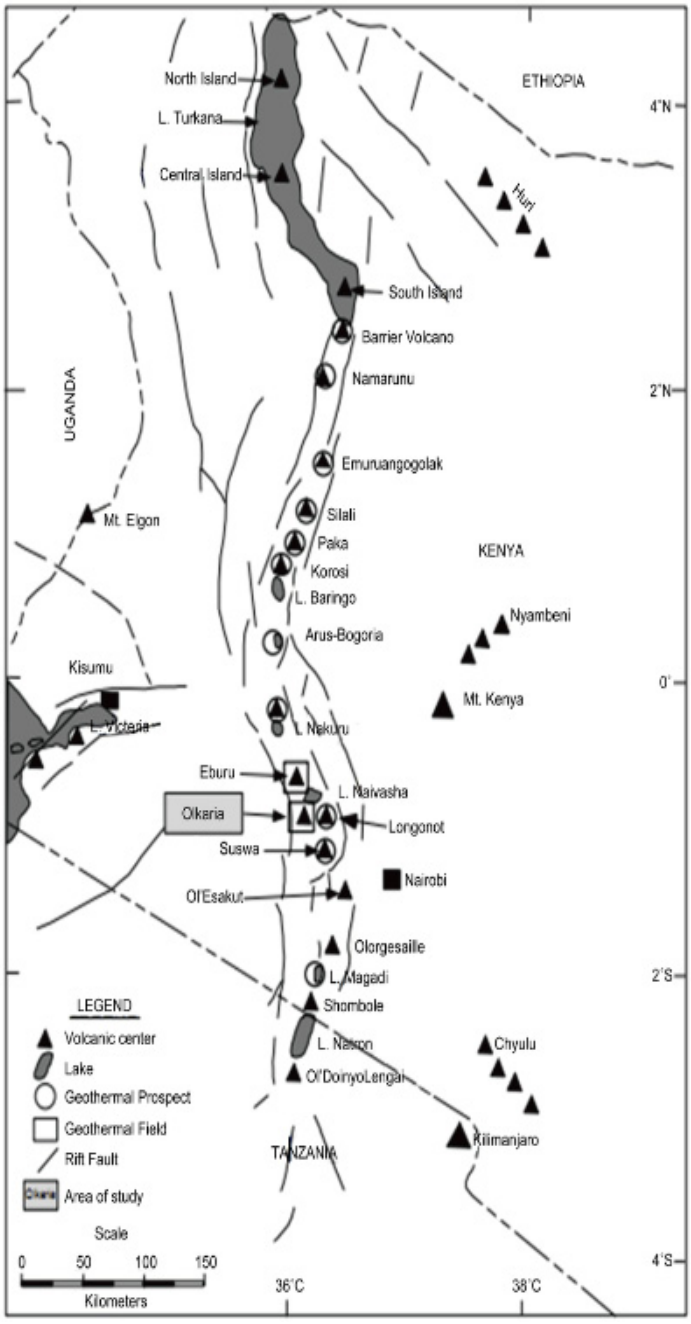

FIGURE 1: Map of the Kenya rift showing the location of the Olkaria volcanic complex and geothermal field and other Quaternary volcanoes along the rift axis (Lagat, 2004)

For ease of geothermal development and management of the Olkaria geothermal field, it has been segmented into seven production sectors: Olkaria East, Olkaria Northeast, Olkaria Central, Olkaria South West, Olkaria North West, Olkaria South East and Olkaria Domes (Figure 2). These sectors are named after Olkaria Hill, a prominent geological feature that is approximately 340 m high and has a basal diameter of 2 km (Ouma, 2009; Koech, 2014).

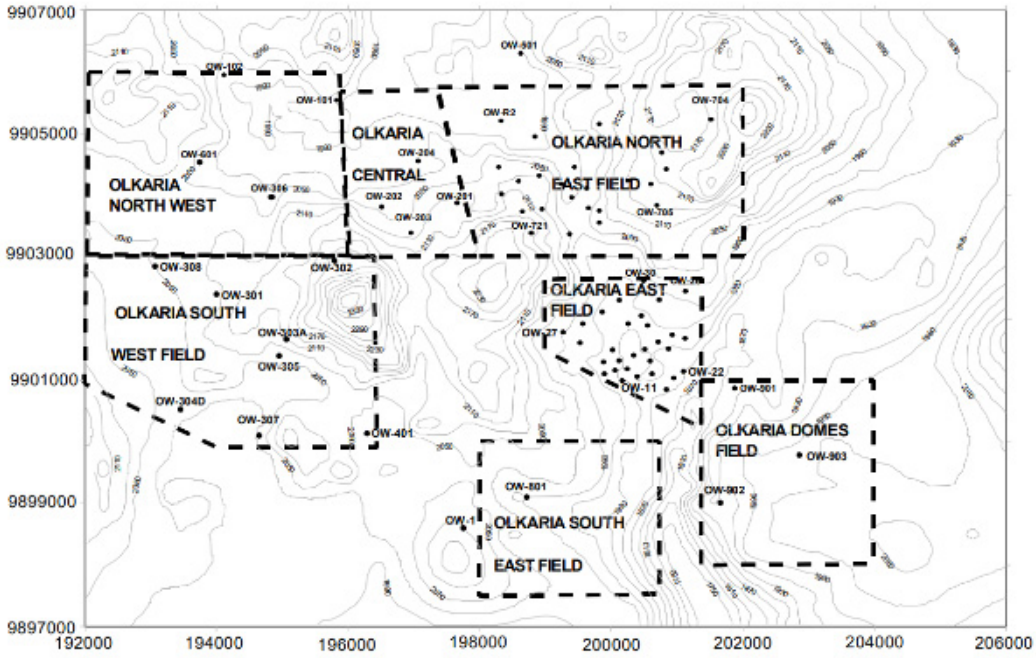

FIGURE 2: Map of the Greater Olkaria Geothermal Area showing the location of the sub-fields. Dots and adjacent numberings indicate wells and corresponding well numbers (Lagat et al., 2005)

2.1.1 Regional and tectonic settings

The Olkaria geothermal field is primarily a volcanic complex and lies south of the central part of the KRS which is part of the eastern branch of the EARS. The eastern branch runs from the Afar Junction in the north to Beira, Mozambique, in the south covering a length of more than 4,000 km (Chorowicz, 2005). EARS is a divergent intra-continental ridge system comprising an axial rift, prelude of oceanic opening, and is situated above two mantle plumes: the Ethiopia and Kenya/Tanzania Domes (Chorowicz, 2005; Bosworth et al., 1998).

Morpho-tectonically, the EARS is controlled by divergent movements that induce localized extensional strain in the continental lithosphere (Chorowicz, 2005). The EARS started with an extension in the north (Red Sea and the Gulf of Aden) about 30 Ma ago (early Tertiary) and propagated south with time. This resulted in the rifting of the African Plate (Nubian plate) from the Arabian plate forming the mantle plumes that developed prior to the continental rupture, thus, there is a close association between doming, rifting and alkaline magmatism/volcanism in the EARS (Saemundsson, 2010; Chorowicz, 2005; Ebinger, 2005; Baker, 1987).

The EARS is a graben that is trough-like, approximately 40 to 65 km wide, and traverses two broad, elongated domal uplifts in Ethiopia and Kenya (Otieno, 2016). Its evolution is attributed to the exploitation of the weak collisional zone within the rift faults at the contact between the Archean Tanzania craton and Proterozoic orogenic belts system, making it structurally controlled (Smith and Mosley, 1993).

The existence of the geothermal system in the area is attributed to magmatic activity (Pleistocene-Holocene) and complex structural patterns that include faults and ring structures (Omenda, 1998). The EARS has formed elongate, narrow rifts due to faulting and subsidence while the lithospheric mantle is subjected to sharply defined ductile thinning, inducing ascension of asthenospheric mantle (Chorowicz, 2005). The KRS opening began with volcanism in the Miocene period when ignimbrite erupted. Thereafter, a faulting episode followed, resulting in the formation of the graben structures known today.

This also resulted in fissure eruptions of trachyte, basalts, and basaltic trachyandesites (Baker et al., 1972; Baker, 1987).

2.1.2 Geology and structural settings

The Kenyan rift, as part of the EARS, evolved though the rifting process with the driving force being provided by convection in the asthenospheric mantle. The rifting resulted in the formation of the young Greater Olkaria Volcanic Complex that is dominated by a peralkaline rhyolite dome and lava field (Marshall et al., 2009).

The Greater OVC is the only area in the KRS where occurrences of comendite have been noted on the surface (Lagat et al., 2005). The exposed lithologic units in OVC consist mainly of volcanic rocks: comenditic lavas-rhyolites, pyroclastics, ashes, pumiceous deposits, and trachytes (Otieno, 2016; Omenda, 1998). Figure 3 shows how the different types of rocks are spread across the OVC. These units originate from various volcanic centres in the area (Kagiri, 1996). The OVC is close to other volcanic centres within the central KRS: Longonot, Eburru and Suswa volcanic centres to the east, north and south, respectively.

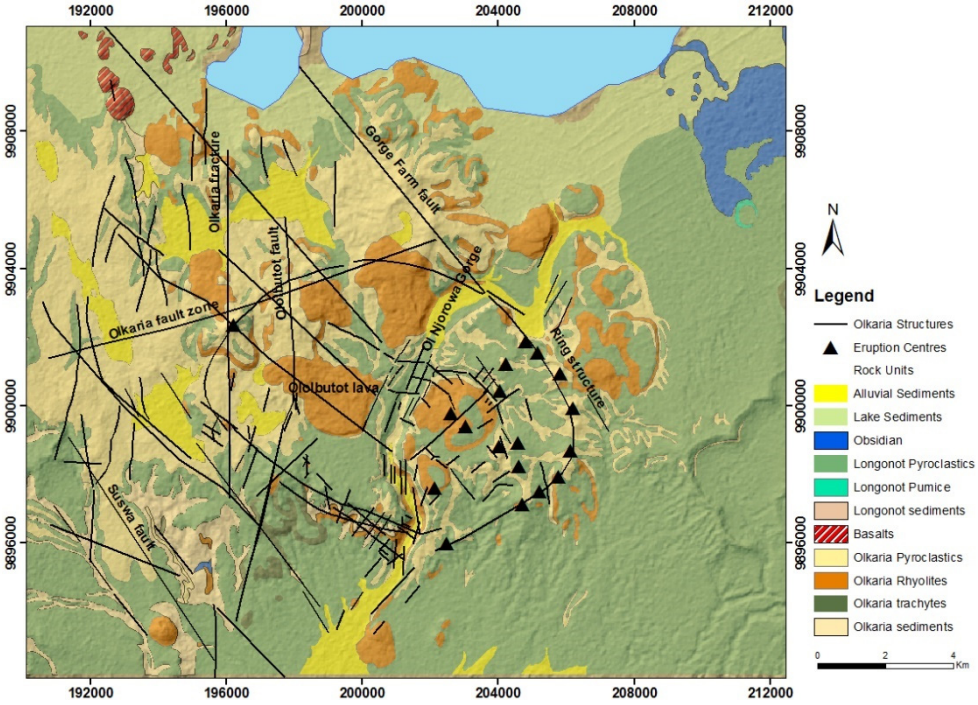

FIGURE 3: Geological map of the Olkaria Volcanic Complex and the surrounding area (Clarke et al., 1990 modified by Munyiri, 2016)

KenGen has drilled over 300 wells in the OVC and this has assisted in revealing part of the subsurface lithostratigraphy of the Olkaria geothermal field. The average drilling depth of wells in Olkaria Northeast field is 2,200-3,000 m with the deepest well being OW-49 at 3,650 m. Most wells drilled after 2013 are around 3000 m deep with a few being less than 2,200 m.

The Olkaria lithological units have been classified into six main groups that vary in age from Pliocene to Holocene, namely: Proterozoic 'basement' formations, Pre-Mau Volcanics, Mau tuffs, Plateau Trachytes, Olkaria Basalts and Upper Olkaria Volcanics (Omenda, 1998; Omenda, 2000; Lagat, 2004). A composite stratigraphic column showing the sub-surface lithotypes of the Olkaria area is shown in Figure 4.

Olkaria well studies have shown that the subsurface stratigraphy is generally composed of rocks that are Quaternary comendites (dominant) with an extensive cover of pyroclastics from the surface to about 600 m depth (from an average elevation of 2000 m a.s.l to about 1400 m a.s.l) (Ofwona, 2010).

The top group forms a superficial layer and overlays the cap rock of the geothermal reservoirs. The cap rock is mainly composed of basaltic lava flows and is called the Olkaria Basalt Group. This group has also minor amounts of pyroclastics and trachytes, though tuffs in this area appear mainly as thin intercalations. This group is underlaid by other groups as follows: Plateau trachyte, Mau Tuffs, Pre-Mau volcanics and lastly the basement Proterozoic Group (Kandie, 2017). This was summarized by Kandie (2017) as shown in Table 2.

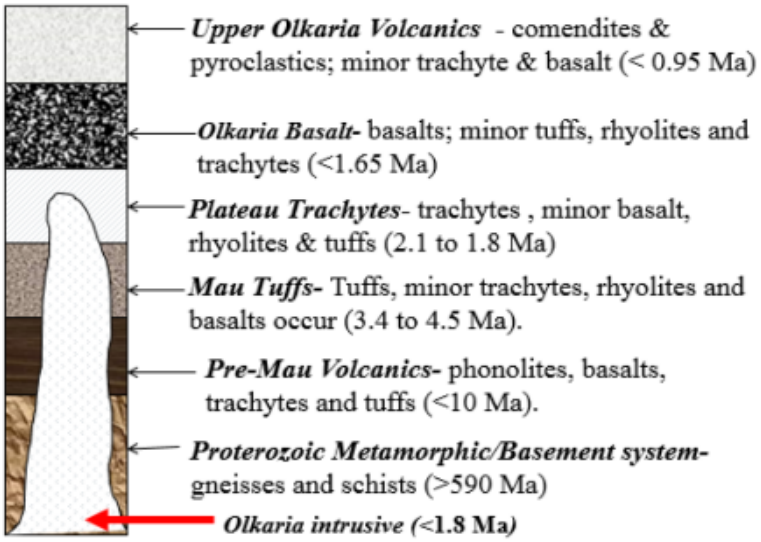

FIGURE 4: Sub-surface lithotypes of the Olkaria Volcanic Complex (Omenda, 1998 modified by Otieno, 2016)

TABLE 2: Summarized stratigraphic groups of the Olkaria formations (Kandie, 2017)

No.	Group	Lithology	Depth (m)	Characteristics
1	Upper Olkaria	Comendite lavas and their pyroclastic equivalents, ashes, minor basalts	Surface-500 m	Superficial
2	Olkaria basalt	Basalt flow, minor pyroclastics and trachytes	100-500	Cap-rock
3	Plateau trachyte	Trachytes with minor basalts, tuffs and rhyolites	1000-2600	Reservoir
4	Mau tuffs	Consolidated ignimbrites	>2600	Reservoir
5	Pre-Mau volcanics	Trachytes, basalts, ignimbrites	unknown	Reservoir
6	Proterozoic	Gneisses, schists, marbles and quartzites	5000-6000	Basement

Geological structures within the greater Olkaria Volcanic Complex include the ring structure, rift fault systems, the Ol-Njorowa gorge, and dyke swarm (Wamalwa et al., 2016) with the most recent structures being the N-S Ololbutot eruptive fissure and the NNE-SSW faults (Mungania, 1999). The arcuate alignment of the domes in the eastern part of the OVC is another important structure as it could indicate the presence of a buried caldera (Naylor, 1972; Clarke et al., 1990; Mungania, 1992).

Most of the faults in the OVC trend ENE-WSW, N-S, NNE-SSW, NW-SE and NNW-SSE (Omenda 1998) and are more prominent in the East, Northeast and Olkaria West fields though not visible in the Olkaria Domes area, possibly due to the thick cover of pyroclastics on the surface. The Gorge Farm fault, which bounds the geothermal fields in the North-eastern part and extends to the Domes area, is the most prominent of the oldest faults that are associated with the development of the rift (Lagat 2004).

The ENE-WSW trending Olkaria Fault (northern slopes of the Olkaria Hill) is one of the two major visible faults that control fluid flow in this region. The other most important permeable structure is the

Ololbutot Fault trending in the N-S direction (Kagiri, 1996). These two major faults intersect the field eastwards, but there are other localized structural lineaments traversing the field in NE-SW and E-W directions. The Olkaria fault cuts through the OVC and is interpreted as an old, rejuvenated structure. It has a lot of geothermal manifestations covering wide areas (widths of 50-100 m) of highly altered grounds (sulphur encrustations and intense silicification) and high-temperature (boiling) fumaroles (Omenda, 1998). Other concealed faults within the OVC are inferred from drill cuttings and cores recovered from wells and stratigraphic correlation (Kagiri, 1996) while other NW-SE trending faults have mostly been inferred from aerial photos and the volcanic centres' alignment (Omenda, 1998; Mwania et al., 2013).

2.1.3 Olkaria hydrogeology

The hydrogeology of the central to southern part of the rift valley is mainly controlled by the rift flanks faults, the grid faulting, and the tectono-axis along the rift floor (Clark et al., 1990). In the OVC, the hydrology is influenced by cold water systems (both at the surface and subsurface) and from geothermally induced flows (Kagiri, 1996). Recent tectonic movements have created enhanced permeability in the Kenyan Rift System by modifying the fracture patterns of the pre-Holocene faults that largely control the region's hydrogeology (Omenda, 1998). Through well monitoring, it is known that geothermal fluid flows from North to South, a trend that corresponds to the orientation of most structures in the geothermal field (Mwania et al., 2013). The Olkaria field has four (4) fault systems that characterize it and control the fluid movement. These are the ENE-WSW, NW-SE, N-S, E-W structures (normal faults) like Ololbutot fault, Olkaria fault, Olkaria fracture, Gorge Farm fault, the ring structure and Ol'Njorowa Gorge (Lagat, 2004).

The OVC reservoir is bounded by arcuate faults that form a ring or caldera structure. Deep-level intrusions inside the ring structure are the main source of magmatic heat. The geothermal reservoir in the north part of Olkaria is liquid-dominated and has no steam-cap. In the south, the reservoir is hosted mainly by trachytic rocks, is two-phase, liquid-dominated, and overlain by a thin steam-dominated zone 100 to 200 m thick at 240°C. The geothermal fluid there has a general composition of 85:15 steam to water ratio and is thus suitable for electrical power generation (Omenda, 1998; Ouma, 2009). This steam dominated zone becomes thinner in the north but thickens in the south. Below the steam zone is a two-phase system of boiling water, while above it is the cap rock that marks the top of the reservoir (Ouma, 2005).

The vertical extent of the OVC reservoir is believed to be at the order of several hundred meters (Bödvarsson and Pruess, 1984). This can be seen in the well lithologies where trachyte, which is the basic reservoir rock, extends up to 1500 m vertically in some wells in the geothermal field. Temperatures measured in wells are generally high, over 250°C, with bottom hole temperatures of about 300°C (Ouma, 2005). According to Ouma (2005), the initial static water level in the OVC varies between 400 and 700 m, depending on location. The initial pressure and temperature distribution in the field reveal that the pressure and temperature increase northwards. The hydrological gradient thus indicates that water movement in the natural state is from north to south. This has been confirmed through drilling for the northern parts of the field where the bottom-hole temperature in most wells exceeds 310°C. The fact that the steam zone, that is present in the Olkaria East field, is replaced by a shallow two-phase zone in the Olkaria Northeast field at almost the same well depth also supports this (Ambusso and Ouma, 1991).

In the updated Olkaria conceptual model (Figure 5), it is assumed that a deep-seated magma chamber or chambers are the heat source in the OVC. The heat is channelled upwards by three main intrusions that are believed to extend up from the magma zone to depths of 6 – 8 km. These possibly partially molten heat source bodies are proposed to lie beneath Olkaria Hill (Olkaria West), in the northeast beneath the Gorge farm volcanic centre, and in the Domes area (Okoo et al., 2017).

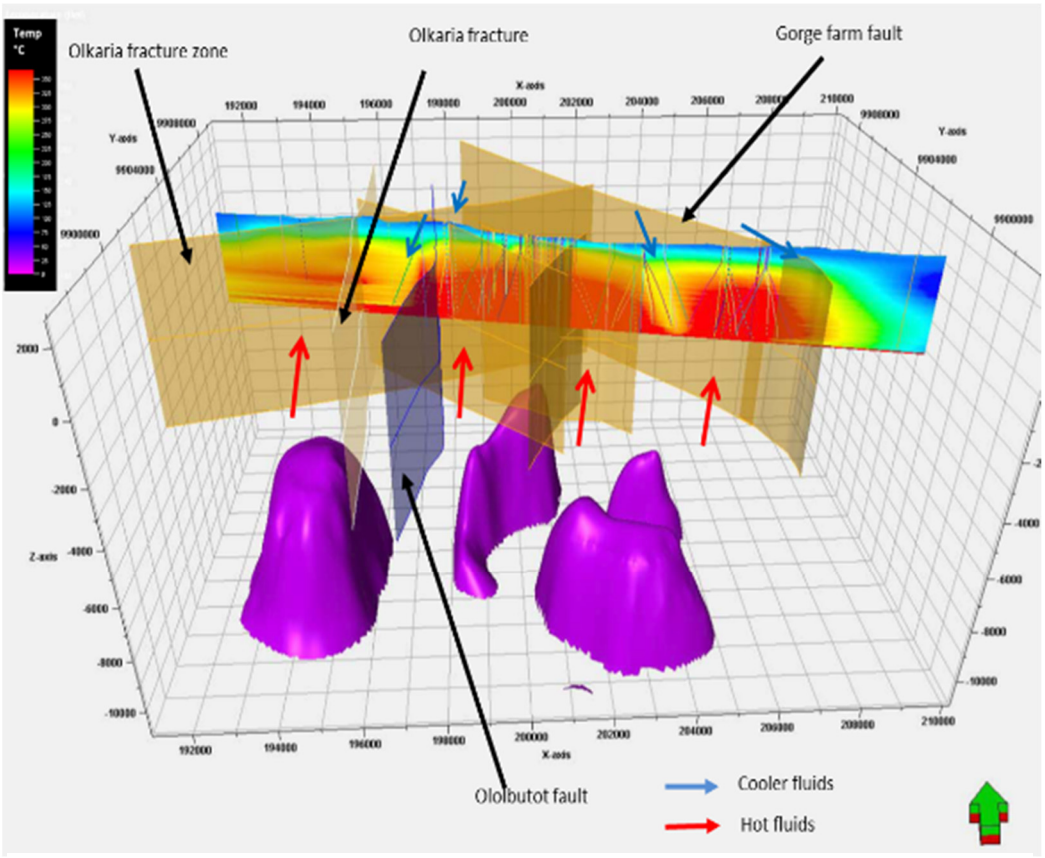

FIGURE 5: Olkaria conceptual model showing the main intrusions in purple and a temperature cross-section (modified from Okoo et al., 2017)

Olkaria has six major geothermal up-flow zones that are spread across the different sectors in the field: East, Northeast, Domes, West, Southeast production fields and the region of well OW-101 (Central and Northwest production fields) (Okoo et al., 2017). These zones are identified through the comparison between alteration and formation temperatures.

The up-flow zone feeding the West field seems to be associated with the Olkaria Hill heat source body. The two up-flow zones, one feeding the Northeast field and another feeding the East field and the northwest corner of the Domes, are probably both associated with the heat source body beneath the Gorge Farm volcanic centre. The up-flow zone that appears to be associated with the ring structures in the southeast corner of the Domes field is related to the heat source proposed beneath the Domes area (Okoo et al., 2017).

Permeability in the OVC is both primary and secondary and is associated with fractures, lithologic contacts between lava units and tuffs, thermally induced joints, clast-matrix, and fragment contacts in breccias and scoraceous fragments (Mwania et al., 2013; Kagiri, 1996). The thermal energy in the fluids in the Olkaria field is mainly transported via convection within the field. This convective flow has been identified from well logs (Lagat, 2004).

Studies suggest that the main source of recharge for the geothermal system could be meteoric water from the Mau escarpment in the west, though the eastern Kinangop escarpment and rift-axial fluid flow could also be important (Naylor, 1972; Ogoso-Odongo, 1986; Clarke et al., 1990; Ojiambo and Lyons, 1993; Bödvarsson, 1993; Omenda, 1994). The annual rainfall in the vicinity of the field is 150 million m^3 and permeates through the N-S oriented structures in the area that include faults and fractures (Bödvarsson, 1993). Figure 6 shows some of these hydrological features in the Olkaria East, Northeast, Central and Domes sub-sectors of the Greater Olkaria Geothermal field.

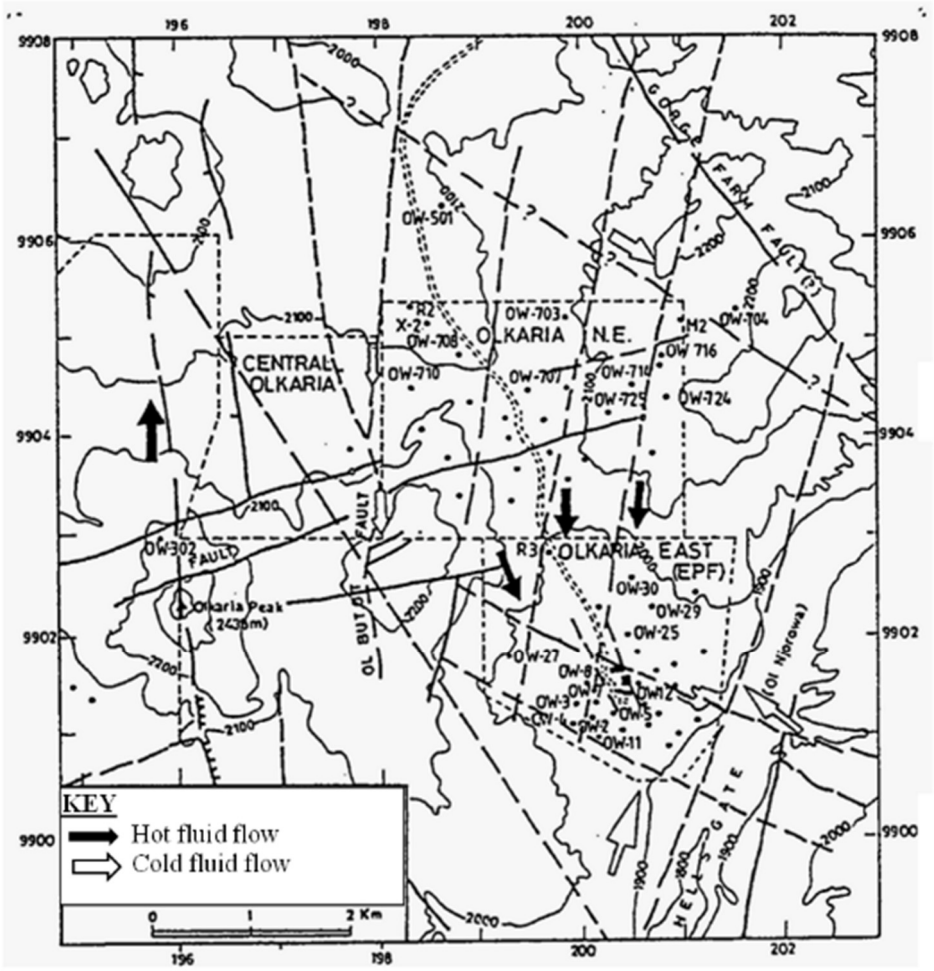

FIGURE 6: Map showing major hydrological features and wells location in the Olkaria East, Northeast, Central and Domes sub-sectors of the Greater Olkaria Geothermal field (Kagiri, 1996)

The regional groundwater flow in the Olkaria area is southwards from Lake Naivasha in the north (KPC, 1981). Deep inflow of cooler recharge fluid into the reservoir in the Eastern part of OVC seemingly occur along the Gorge Farm fault in the northeast and along the fracture zone in Olkaria Central between Ololbutot fault and Olkaria Hill. In the northern part of the OVC, however, the regional groundwater flow into the geothermal system seems to be mixing with hot water flowing from the up-flow zone (Ofwona, 2002)

The geothermal fluids in Olkaria have relatively low concentration of total dissolved solids (TDS) in comparison to other high-temperature wells in the world (Karingithi, 2000). Chemical analysis of fluids from the OVC suggests that the reservoir fluid originates from a deep source of at least 340°C. Secondary fluids are formed during upwelling, boiling and steam separation, particularly in the upper two-phase zone (Ofwona, 2010).

2.2 Role of re-injection in resource management

Geothermal energy is usually considered a green energy due to its renewability and its minimal effect on the environment. Long-term production capacities of geothermal systems are controlled by several factors such as the size, energy content, permeability structure, boundary conditions and re-injection management of the geothermal system (Axelsson, 2013c). In general, sustainable geothermal utilization

is achieved by incorporation of best practices in reservoir management. These include well-balanced energy efficient utilization programs, re-injection strategies and carefully planned monitoring programs (Montanari et al., 2008).

Re-injection is the process of returning, wholly or partially, the extracted energy-depleted fluids back into the geothermal system through specific wells known as re-injection wells. Geothermal re-injection started about 50 years ago in Ahuachapan, El Salvador, in 1969, at The Geysers in California in 1970 and in Larderello, Italy, in 1974 (Axelsson et al., 2005). It started as a means of waste disposal but has now become an integral part of many geothermal operations in the world (Axelsson, 2008).

In the early 1980s, re-injection became imperative after its implementation was tested in several fields and considerable positive impact was noted on the environment and energy recovery (Kamila et al., 2021). Later, other geothermal operators adopted the policy of injecting water of different origins into geothermal reservoirs to improve the geothermal reservoir performance (Axelsson, 2008). Re-injection has been embraced in many geothermal fields and is currently practised in over 90 geothermal fields in at least 25 countries (Axelsson, 2008; Kamila et al., 2021). Re-injection is not only a means of geothermal waste-water disposal and pressure support but can also assist in maximising thermal extraction from reservoir rocks and can revitalize surface features like hot springs and fumaroles (Axelsson, 2013c). However, geothermal fields have unique thermodynamic states, geological settings, and reservoir characteristics, and thus optimization of re-injection strategies is complicated and must be undertaken carefully to maximize its benefits (Diaz et al., 2015; Kaya et al., 2011).

Re-injection can be done in three possible areas. This can be areas that are completely outside the main production field, within the main production area (in-between the production wells) or just within the periphery of the main production area (but still in direct hydrological connection) (Axelsson, 2008). To decide on the best reinjection strategy for any geothermal field, it is important to evaluate each field individually. This is done by first identifying the dominant depletion mechanisms in each type of geothermal system. Note that geothermal systems can be grouped broadly into three types: two-phase, vapour-dominated systems (VDS), two-phase, liquid-dominated systems (LDS) and hot-water systems (HWS) (Diaz et al., 2015). Additionally, the re-injection sites are usually chosen based on the purpose or function of the re-injection. If the aim of the re-injection is to provide pressure support, then the re-injection well should be sited in between the production wells or alternatively in the periphery and at greater depths below the main reservoir, but if it is just for environmental reasons then the well can be sited either in a production depth range or at shallower or deeper levels outside the main production field. Re-injection wells meant for pure waste disposal do not need to have a direct hydrological connection to the production reservoir (Axelsson, 2008). Therefore, in VDS, it may be useful to re-inject water infield as these reservoirs tend to run out of water while the rock matrix still contains sufficient heat for use in geothermal utilization (Diaz et al., 2015).

Natural geothermal reservoirs are classified as either open or closed, depending on their boundary conditions and what their long-term behaviour is like. In closed systems, pressure declines continuously with time, and at a constant production rate their production capacity is limited by the quantity of fluid rather than the available thermal energy. In open systems, the pressure stabilizes as recharge into the system eventually reaches an equilibrium with mass extraction. The recharge may be hot, deep recharge and/or cold, shallow recharge. With time cold shallow recharge can cause the reservoir temperature to decline. The production potential of open systems is, therefore, often limited by reservoir energy content and not the geothermal fluid (Axelsson, 2013c). Therefore, the boundary type is a factor that influences the re-injection strategy.

Despite the positive impacts of re-injection discussed above, it is still known to causes negative effects on production in a geothermal field if not well managed. These effects include chemical or thermal breakthrough, boiling suppression, ground lifting, subsidence, induced micro-seismicity, rapid aquifer clogging, scaling and corrosion in surface pipelines and re-injection wells (Axelsson, 2013a; Kamila et al., 2021).

2.2.1 KenGen´s historical reinjection strategy in Olkaria

Numerical modelling was carried out for the Olkaria geothermal system after production had started in the early 1980s to assess the field´s generating capacity. It was noted that there was a decline in deliverability of production wells with time and monitoring of the production wells was recommended to estimate the decline rate (Bödvarsson and Pruess, 1981). Further numerical simulation studies were undertaken later, which suggested that re-injection into the field should be implemented as it would reduce well decline rates and therefore reduce the number of make-up wells required (Bödvarsson and Pruess, 1984; Bödvarsson, 1993).

This steam decline became apparent in 1985 when the field started experiencing pressure drawdown that resulted in declining well outputs and thus declining steam supply to Olkaria 1, then the only geothermal power plant in the area. The decline in pressure also caused severe cyclicity in some of the wells in Olkaria East (Ouma, 1992). This necessitated the drilling of several make-up wells to try to maintain the steam demand of the power plant (Ouma, 2009).

Re-injection strategies for the Olkaria geothermal fields were discussed at length as it was found to be more economically favourable than the drilling of new wells. This led to the implementation of cold and hot re-injection in the field starting in 1993 (Ouma, 2009). For the strategic re-injection to be successful, KenGen has drilled several re-injection wells in Olkaria, over time. There are currently 40 hot and cold re-injection wells that are distributed across the field and receive both geothermal brine and steam condensate from wells, separators and power plants in the area (Table 3).

It is important to note that the Olkaria Northeast Production Field (ONEPF) fully supports the 105 MW_e Olkaria 2 power plant, partially the 140 MW_e Olkaria 1AU (Units 4 and 5) power plants, as well as supplying geothermal fluid to the Olkaria Geothermal Spa (Kandie, 2017). The northeast production field has been exploited for over 17 years and its neighbour the Olkaria East Production Field (OEPF) has been exploited for 40 years. The OEPF supplies steam to both Olkaria 1 (45 MW_e) and to Olkaria 1AU (140 MW_e) power plants. Other power plants and wellheads are also in operation in other parts of these fields.

TABLE 3: Re-injection wells in Olkaria

East Production Field	Northeast Production Field	Domes Production Field
OW-12 (hot)	OW-718 (hot)	OW-906A (hot)
OW-13 (hot)	OW-R2 (hot)	OW-911 (hot)
OW-17 (hot)	OW-703 (hot)	OW-911A (hot)
OW-34 (hot)	OW-708 (hot)	OW-913A (hot), OW-928 (hot)
OW-03 (hot)	OW-739R1 (cold)	OW-902 (hot), OW-917 (cold)
OW-07 (hot)	OW-R1 (cold)	OW-901 (hot), OW-912B (hot)
OW-21 (hot)	OW-X2 (cold)	OW-919 (cold), OW-922 (cold)
OW-R3 (hot)	OW-201 (cold)	OW-902A (cold)
OW-801R1 (cold)	OW-204 (cold)	OW-902B (cold)
OW-801R2 (cold)	OW-X1 (not in use)	OW-R10 (cold)
OW-R4 (both hot & cold)	OW-R11 and OW-R12 (Both cold)	OW-R9 (cold)
OW-R5 (both hot & cold)	OW-723A (hot)	OW-R8 (cold)
OW-11 (hot)	0W-711 (hot)	OW-R7 (cold)

Note that in the Olkaria Northeast field we currently have 100% reinjection of effluent generated by the production wells (both cold condensate and hot brine from Olkaria II Power plant are re-injected into the system). Hot brine is re-injected into wells OW-R2, OW-R3, OW-703 and OW-708 whereas cold condensate is re-injected into well OW-201 and well OW-204 (Ouma, 2005).

The first chemical tracer and cold-injection test in Olkaria was done in 1993 by injecting lake water into well OW-03 and later 125 kg of sodium fluorescein (Ambusso, 1994). This was done to find out whether there were some direct connections between wells in the geothermal field. Over 400,000 m^3 of water was injected into the well over a period of 172 days. The chemical tracer was injected 45 days after the start of the injection. The test confirmed several well connections in the field. Production and chemical changes were observed in wells OW-2, 4, 7, 8, 10 and 11. It was, therefore, shown that well OW-03 had connections, possibly fractural, with wells OW-02, 04, 07 and 11. Simulation studies had also shown connections to wells OW-05, 07 and 08 (but not OW-02 and 11) (Ofwona, 1996). This well was converted into a hot water re-injection well in May 1995 (Ouma, 2009).

To confirm the suitability of well OW-704 for waste-brine re-injection and reduce the well engineering design uncertainty, tracer and injection tests were performed in the Northeast Field in 1993/1994 using two different tracers on separate dates (Karingithi, 1994). First, 250 kg of sodium fluorescein dye was dissolved in 4000 litres of water and injected into the well as a slug. The tracer returns were monitored and observed in wells OW-M2, OW-704 and OW-716. The other two wells on discharge (OW-714 and OW-725) did not show any tracer returns. A different chemical tracer, Potassium iodide, was later injected in OW-704 for long term monitoring.

A tracer/injection test was done in well OW-R3 from May 1995 to July 1996. Cold lake water was continuously injected into the well at an average rate of 100 ton/hr (27.8 kg/s). 500 kg of sodium fluorescein tracer was then introduced as a slug after 27 days of injection. Wells close to OW-R3 were monitored for chemical and output changes. However, very little tracer returns were measured in wells OW-25, OW-29 and OW-30 and none in the closest wells, OW-32 and 34. There was also very little or no change in the fluid chemistry and production output from the neighbouring wells (Ofwona, 2005).

Tracer tests have been performed at least twice in well OW-12, in 1996 and in 2016. Well OW-12 was a production well in a high temperature zone with very good injectivity but had experienced pressure decline before it was converted to a re-injection well in 2015 (Mwawongo, 2004). In 1996, 500 kg of sodium fluorescein was injected into the well. This was after 20 days of cold-water injection at a rate of 100 ton/hr. A total of 137,000 tonnes of cold water was injected into the well over 416 days. Wells OW-15, 16, 18 and 19 showed strong connections to OW-12 (Ofwona, 1996; Ofwona, 2005). Monitoring of these wells indicated improvement in mass output with reduced enthalpy due to cold re-injection. Therefore, cold injection was discontinued to enable the affected wells to recover (Ofwona, 2002). Based on modelling work involving the well, Koech (2014) noted that OW-12 could be used intermittently as a cold reinjection well (injection for one year followed by a period of recovery). The well was later converted into a hot re-injection well (Ofwona, 2002). However, it still has high well pressure that hinders it from taking in brine smoothly. It was meant to receive brine from Olkaria wells OW-20, 24, 25, 26, 28 and 32.

In 2016, 200 kg of sodium fluorescein was injected into well OW-12. Background studies were done for 23 weeks in the surrounding wells and after that production monitoring was done for about 6 months. At least 15 wells within the OEPF and ONEPF showed a connection to well OW-12, six of these showing a strong to moderate connection. These six wells were OW-14, 15, 16, 19, 22 and 38B (Koech et al., 2017). In 2016, another well at the Domes, well OW-906, was also injected with sodium fluorescein tracer. Tracer returns were noted in well OW-926A and eleven other wells in the Domes field. These were wells OW-903, 903A, 904, 904A, 904B, 908, 910, 910B, 912A, 915 and 916. Sodium fluorescein was injected into well OW-902 in mid-2018 and fifteen production wells were monitored until January 2019. No tracer was recovered from any of the monitoring wells.

In February 2019, sodium fluorescein tracer was injected into well OW-34 and the wells in the field were monitored for six months. The tracer results showed some connections between well OW-34 and 12 other wells. These included wells OW-20, 24, 27, 28, 31, 33, and 35. These wells are largely controlled by two NW-SE trending faults that dissect the recent Ololbutot lava flow (Wamalwa and Nyawir, 2020a). In mid-2020, 400 kg of sodium fluorescein was injected into well OW-928 after

background studies had been done for about a month for 33 of the surrounding wells. Forty-one production wells were thereafter monitored for the tracer for about 6 months. Over 90% of the monitored wells at the Domes showed tracer returns. These included wells OW-901A, 901B, 903A, 905, 907B, 908, 908A, 909A, 910A, 910B, 912D, 914, 914B, 915, 915C, 915D, 916B, 921, 921A, 923B, 923C, 925, 925A, 925B and 926B. It was noted that the fluid flow paths in the Domes Field appear to be controlled by the NW-SE and NE-SW faults (Wamalwa and Nyawir, 2020b).

Finally, it should be mentioned that tracers were also added in 2004 to the fluid re-injected into well OW-708 with returns reported in OW-706 and OW-712. Tracer tests have also been done involving well OW-R2 (in 2004) in the Olkaria Northeast field (Karingithi, 1994; Ofwona 2002; Ofwona, 2005; Ouma, 2005).

2.3 Geothermal tracer testing, purpose, and interpretation

2.3.1 Geothermal tracer testing

Tracer testing is a powerful research tool for studying and understanding fluid flow paths, which helps when setting up re-injection strategies (Axelsson, 2013a). Tracer tests involve injecting a known chemical tracer into a hydrological system and thereafter monitoring the tracer recovery through time at various observation points. These observation points are, in most cases, other wells and/or springs. The results obtained can be used to study flow-paths and to quantify the flow (Axelsson, 2013a). Tracer testing is, therefore, an indirect method for characterizing the subsurface hydrological systems. Its success rate depends on the planning prior to execution (Sverrisdóttir, 2016). Other than in the geothermal energy sector, tracer testing has been used in several industries including ground water hydrology, nuclear waste storage studies, petroleum engineering and pollution studies.

2.3.2 Tracer testing purpose

The purpose of geothermal tracer testing is threefold: (1) For general hydrological studies of subsurface flow, (2) for re-injection research and management, and (3) for flow rate measurements in pipelines carrying two-phase water mixtures (Axelsson, 2013a). Moreover, tracer tests results can also be used as the basis for calculating cooling predictions for a geothermal reservoir, as well as to provide information on other reservoir characteristics (Axelsson, 2008). This information is key in re-injection strategies (siting of re-injection wells) and for overall sustainable management of the geothermal resources.

2.3.3 Tracer test design

Tracers can either be naturally occurring in geothermal fluids or artificial. Natural tracers include various stable water isotopes, chloride, iodine and even ammonia. Artificial tracers used in the geothermal industry are grouped into three major types: liquid-phase, steam-phase, and two-phase tracers (Axelsson, 2013a). Axelsson et al. (2005) describes several aspects that need to be considered when designing a tracer test: (1) what tracer to select, (2) the amount of tracer to inject and (3) the sampling plan to follow (sampling points and frequency). The selected tracer must meet some basic criteria. According to Axelsson (2013a) and Kamila et al. (2021), tracers should:

i. Not be present in the reservoir or if present, then their concentration should be much lower than the expected concentration of the tracer to be injected,
ii. Not react with or be absorbed by reservoir rocks
iii. Be thermally stable at reservoir conditions
iv. Be relatively inexpensive
v. Be easy (fast/inexpensive) to analyse
vi. Be environmentally friendly
vii. Be able to adhere to prevailing phase (steam or water) conditions

viii. Degrade/decay slowly with time, so that they do not leave a long-lasting signature that impacts the outcome of possibly future tracer testing

Sodium-fluorescein is a fluorescent dye that has been used successfully in numerous low- and high-temperature geothermal fields and meets most of the criteria listed above. It is commonly used in monitoring liquid phases for flow-rate measurements in two-phase pipelines. However, it is known to decay at temperatures above 230°C (Axelsson, 2013a). According to a detailed study by Adams and Davis (1991), the sodium fluorescein thermal decay becomes significant above 200°C. The half-life of fluorescein is 150 and 37 days at 220 and 240°C, respectively. Above 250°C, it decays too rapidly for it to be used as a tracer. However, fluorescein tracer tests in high-temperature geothermal systems may, in principle, be corrected for this decay if the temperature along the flow path between injection and production wells is known (Axelsson et al., 2005).

Before carrying out any tracer injection in a geothermal field, it is preferable to ensure that the geothermal reservoir is in a pressure-stable state. This prevents major transients in the flow-pattern of the reservoir, making the data analysis easier. In most cases, a tracer is injected into the targeted borehole over a very short period which can be considered instantaneous (Axelsson, 2013a).

Following this, a draft of a sampling schedule containing both the sampling frequency and the sampling points is developed. During the testing period the sampling frequency should be adjusted depending on the results obtained (Sverrisdóttir, 2016). Tracer returns can be observed in monitoring wells based on their connectivity to the injection well. In cases where tracer breakthroughs are observed, the breakthroughs are either fast, intermediate, or slow. Figure 7 shows this schematically. Tracer analysis samples are most often collected from flowing/producing boreholes. However, in cases where samples from non-discharging wells are required, down-hole sampling may be used (Axelsson, 2013a).

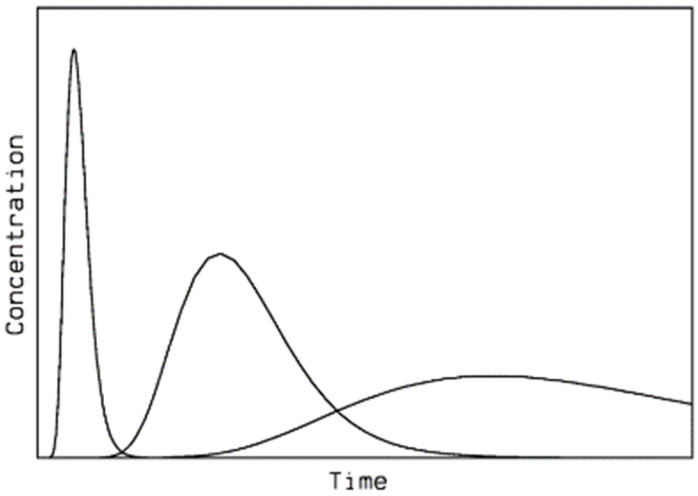

FIGURE 7: Typical fast, intermediate, and slow tracer return profiles (Axelsson et al., 2005)

Sampling of geothermal fluids for the injected tracer usually lasts for a few weeks, months or even years. The length of this period depends on the tracer injected, the local reservoir conditions and distances between wells, which control the fluid flow-pattern in the reservoir. These conditions control when and where the tracer return peaks will be seen (Axelsson et al., 2005). The frequency of sampling is case specific but should, generally, be higher in the first week, preferably twice a day. This frequency should decrease with time and be around twice a week during the last weeks of monitoring. Higher tracer returns are usually expected in the beginning due to tracer dispersion over time. However, the sampling frequency is often affected by technical restrictions such as available manpower, the number of wells being sampled, measurement techniques and other factors and can be cut short for technical and financial reasons (Axelsson et al., 2005).

Once the re-injection site (a borehole) has been identified, several factors need to be considered in determining the amount of tracer that will be needed (Axelsson et al, 2005). These factors include the tracer detection limit, background values, injection rate (q), the number of production wells and their production rate (Q), distances involved and anticipated return rate (slow/fast depending on the distances

involved and how directly the wells involved are connected). The required mass can also be estimated through mass-balance calculations.

2.3.4 Tracer data interpretation

The TRINV software, included in the ICEBOX geothermal software package (Arason et al., 2004), has been used for the simulation of tracer recovery data. The software has been successfully used in several geothermal systems to analyse tracer test data by modelling the tracer recoveries and calculating cooling predictions for the systems. It has e.g. been used in Laugaland in Iceland, Ahuachapan in El Salvador, the Philippines, Indonesia, and China. Tracer interpretation models are governed by the theory of solute transport in porous/permeable media which incorporates transport by advection, mechanical dispersion, and molecular diffusion (Axelsson et al., 2005). It is on this basis that the computer software (TRINV) was developed to estimate (invert for) flow characteristics of the flow channels by using an automatic inversion technique to simulate tracer return profiles. The model assumes that there is a specific flow channel(s) connecting the injection boreholes with production boreholes, thus, it simulates the tracer transport based on that. This one-dimensional flow in a flow-channel is illustrated in Figure 8. The interpretation results are consequently used during long-term re-injection to predict temperature decline and thermal breakthrough (Axelsson et al., 2005).

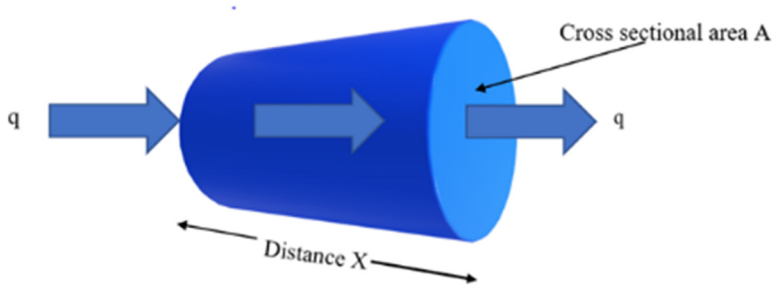

FIGURE 8: A schematic figure of a flow-channel with one-dimensional flow (modified from Axelsson et al., 2005)

One can visualize the flow channels as parts of near-vertical fracture-zones or horizontal interbeds or layers and that the flow channels are delineated by the boundaries of these structures on one hand and flow-field streamlines on the other hand. However, there can be situations where more than one channel is connecting an injection borehole to more than one feed-zone in a production borehole. Below is the relevant simplified differential equation for the case of one-dimensional tracer transport (Axelsson et al., 2005):

$$D\frac{\partial^2 C}{\partial x^2} = u\frac{\partial C}{\partial x} + \frac{\partial C}{\partial t}. \qquad (1)$$

Here;

D	=	dispersion coefficient (m^2/s) of the material in the flow channel
C	=	the tracer concentration in the channel (kg/m^3)
x	=	the distance along the channel (m)
u	=	the average fluid velocity in the channel (m/s), given by $u = q/(\rho A \varphi)$,
q	=	the injection rate (kg/s)
ρ	=	the water density (kg/m^2)
A	=	the average cross-sectional area of the flow-cannel (m^2)
φ	=	the flow-channel porosity

Molecular diffusion is neglected in this simple model such that $D = \alpha_L u$ where α_L equals the longitudinal dispersivity of the channel. Assuming instantaneous injection of a mass M of tracer at time t = 0, the solution is given by:

$$c(t) = \frac{uM\rho}{Q}\frac{1}{2\sqrt{\pi Dt}}e^{-(x-ut)^2/4Dt}. \quad (2)$$

Here c(t) is the tracer concentration in the production borehole fluid, Q the production rate (kg/s) and x the distance between the boreholes involved. In the equation above, it has been assumed that there will be no loss of tracer. The law of conservation of mass means that $c \cdot Q = C \cdot q$. Equation (2) is the basis for the method of tracer test interpretation presented here, which involves simulating tracer return data with the equation. Such a simulation yields information on the flow channel cross-sectional area Aφ, the dispersivity α_L as well as the mass of tracer recovered through the channel. In the case of two or more flow-channels, the analysis yields an estimate of these parameters for each channel. The flow channel pore space volume, A*x*φ, is estimated through the estimate of the flow channel cross-sectional area Aφ.

One of the main goals of geothermal tracer testing is to predict thermal breakthrough and temperature decline during long-term re-injection. The uncertainty of heat-transfer predictions can be estimated by considering different assumptions of flow-channel dimensions. At least two extremes are considered, an optimistic and a pessimistic model. Pessimistic models assume that the flow-channel has a small surface area or is pipe-like, so heat transfer from the rock is small. For optimistic models, the flow channel has a large surface area, such as thin fracture-zones or thin horizontal layers, with larger heat transfer from the rock. However, in modelling the cooling predictions, additional data, e.g. actual temperature changes, or data of chemical variations, can be used to constrain the cooling predictions (Axelsson et al., 2005).

3. INJECTION OF TRACER INTO WELL OW-703 AND ITS SUBSEQUENT RECOVERY

3.1 Re-injection into Olkaria well OW-703

Olkaria well OW-703 was drilled as the third exploratory well in the northern part of the Northeast Field (commonly referred to as the 700 series) in early 1987. The well is situated at the surface coordinates Northing 9905175.680 and Easting 199810.190, at an elevation of 2089 m a.s.l. Figure 9 shows the location of the well alongside other wells in the geothermal field. The well was drilled following the drilling of wells OW-701 and OW-702 in the same field (Ouma, 2009). Well OW-703 was sited within the geophysical boundary of the Olkaria licence area, and was situated there to further define, delineate, and constrain the geothermal resource north of OW-701 and southeast of OW-501. The well was drilled to a total depth of 2200 m with the production shoe-casing reaching a depth of 741 m. During the drilling of the well, total loss of circulation was experienced between 144 and 741m, and from 1560 m to the well bottom (Muchemi, 1987). Stratigraphically, the well has a lithological sequence similar to the other wells in the EPF and NEPF, i.e. pyroclastics overlaying rhyolites with intercalations of basalt, tuff, rhyolite, and trachyte below the rhyolites.

The hydrothermal alteration intensity in well OW-703 is comparable to other wells within Olkaria, though the well has a higher grade of alteration. The hydrothermal alteration found in the well indicates high temperature conditions with several high temperature minerals observed in the drill cuttings. The first appearance of epidote was noted at 648 m depth. Two epidote peaks were noted at 880-915 m depth and at 1030-1220 m depth. This indicates reservoir temperatures higher than 250°C. Biotite, prehnite and traces of actinolite are noted at a depth of 1375 m (Muchemi, 1987). This indicates paleo-temperatures higher than 300°C. The latest temperature logs measured in 2003 show that the well has a temperature of about 300°C below a depth of 1200 m (Figure 10). The temperature increases with depth and is about 330°C at the well bottom.

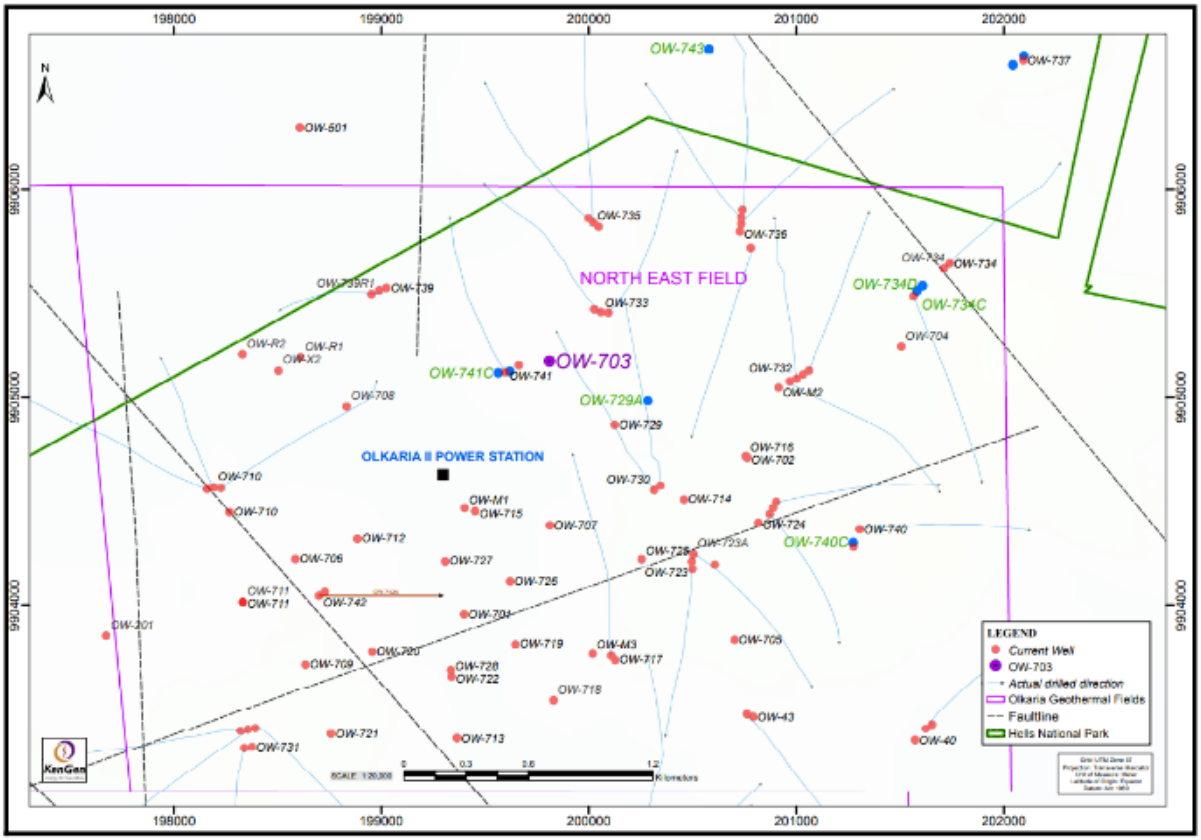

FIGURE 9: Location of well OW-703 in relation to other wells within the NEPF

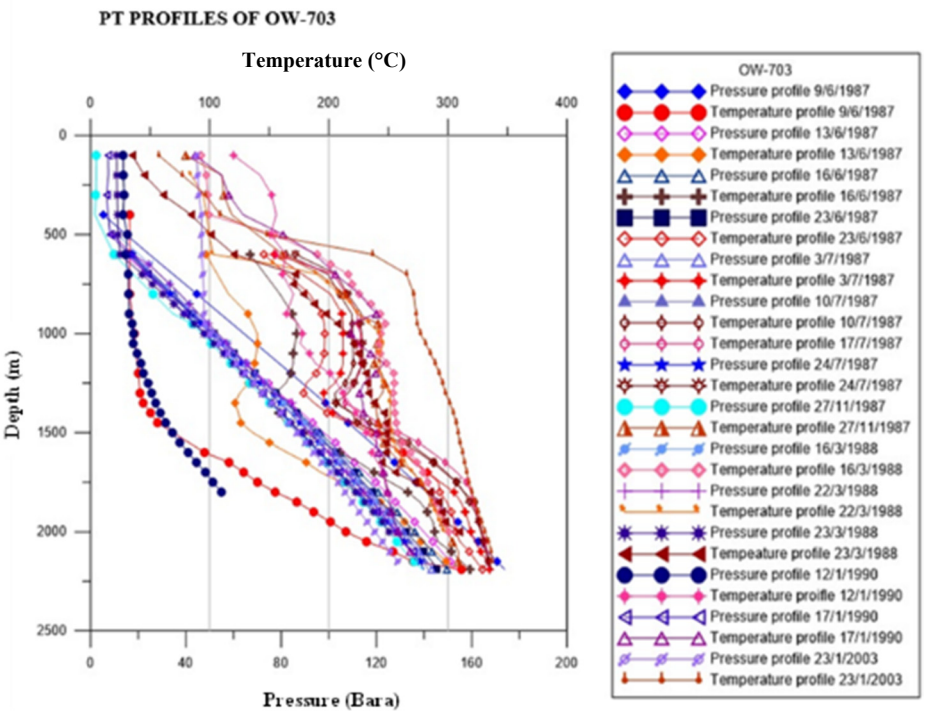

FIGURE 10: Pressure and temperature profiles for well OW-703

3.2 Background sampling of OEPF and ONEPF wells

Prior to the tracer injection, fluid samples were collected from all the production wells in ONEPF and some other wells in the vicinity (in the adjacent OEPF) that were online. Samples were also collected from a weir box at well OW-716, as it was being discharge tested. These fluid samples were used to estimate the baseline sodium fluorescein in the reservoir. These sodium fluorescein baseline values were in the range of 0.03-0.19 ppb in ONEPF and 0.03-0.13 ppb in OEP (Table 4). This was done approximately 3 weeks prior to the tracer injection. The samples were analysed at a temperature of 25°C for pH, conductivity, sodium fluorescein, and chloride concentrations.

TABLE 4: Average results of background measurements for 26 wells in OVC

Well No	pH	Tracer Concentration (ppb)	Chloride concentration (ppm)	Fluid conductivity (ppm)
19	9.66	0.030	581	2490
35	11.1	0.037	1200	5000
37A	10.4	0.073	2110	8570
37B	9.98	0.091	2200	8170
43	9.19	0.065	331	1590
43A	9.19	0.135	324	1630
44	8.91	0.060	1230	4500
44A	7.86	0.035	177	1370
44B	9.74	0.038	1350	5550
701/727	9.71	0.061	655	2710
709	10.1	0.113	777	3600
712	8.80	0.112	38	4960
714	10.1	0.111	500	2610
716	9.97	0.149	485	2490
719	9.70	0.059	465	2270
720/728	10.2	0.119	555	2500
721	10.1	0.172	462	2600
724A	9.83	0.187	324	1920
725	9.85	0.129	451	2450
726	9.71	0.077	650	2650
730A	9.68	0.074	648	2880
730B	9.90	0.030	750	3600
732	9.64	0.044	586	2660
732A	9.85	0.050	555	2500

3.3 Tracer injection

Considering the re-injection rate, average reservoir thickness, porosity, size of the resource area (ONEPF) and the average sodium fluorescein background concentration in the area, the decision was made to inject 550 kg of the sodium fluorescein chemical tracer into Olkaria well OW-703. The tracer injection was done on 14th December 2020 and the recovery monitored until 20th of May 2021. Re-injection well OW-703 is usually fed brine from several nearby wells in ONEPF (Table 5 and Figure 11).

The sodium fluorescein tracer is in powder form and was dissolved in cold water prior to injection into the borehole. For this test, a cementing truck with a mixer was used for dissolving the 550 kg of the tracer in 3,000 L of water. Afterwards, the tracer slurry solution was injected into the well through the wing valve in the shortest possible time to simulate instantaneous tracer injection into the reservoir.

TABLE 5: Wells supplying brine into re-injection well OW-703

Well No	Status	Mass flow (ton/hr)	Mass flow (kg/s)		Well No	Status	Mass flow (ton/hr)	Mass flow (kg/s)
714	Open	94	26.1		732	Open	67	18.6
716	Open	52	14.4		732A	Open	117	32.5
724A	Open	120	33.3		719	Discharge testing	N/A	N/A
725	Open	104	28.9		705	Shut	N/A	N/A
726	Open	30	8.3		717A	Shut	N/A	N/A
730A	Open	23.4	6.5		715	Shut	N/A	N/A
730B	Open	34	9.4		707	Shut	N/A	N/A
		Total Mass Flow into OW-703 in ton/hr						641.4
		Total Mass Flow into OW-703 in kg/s						178

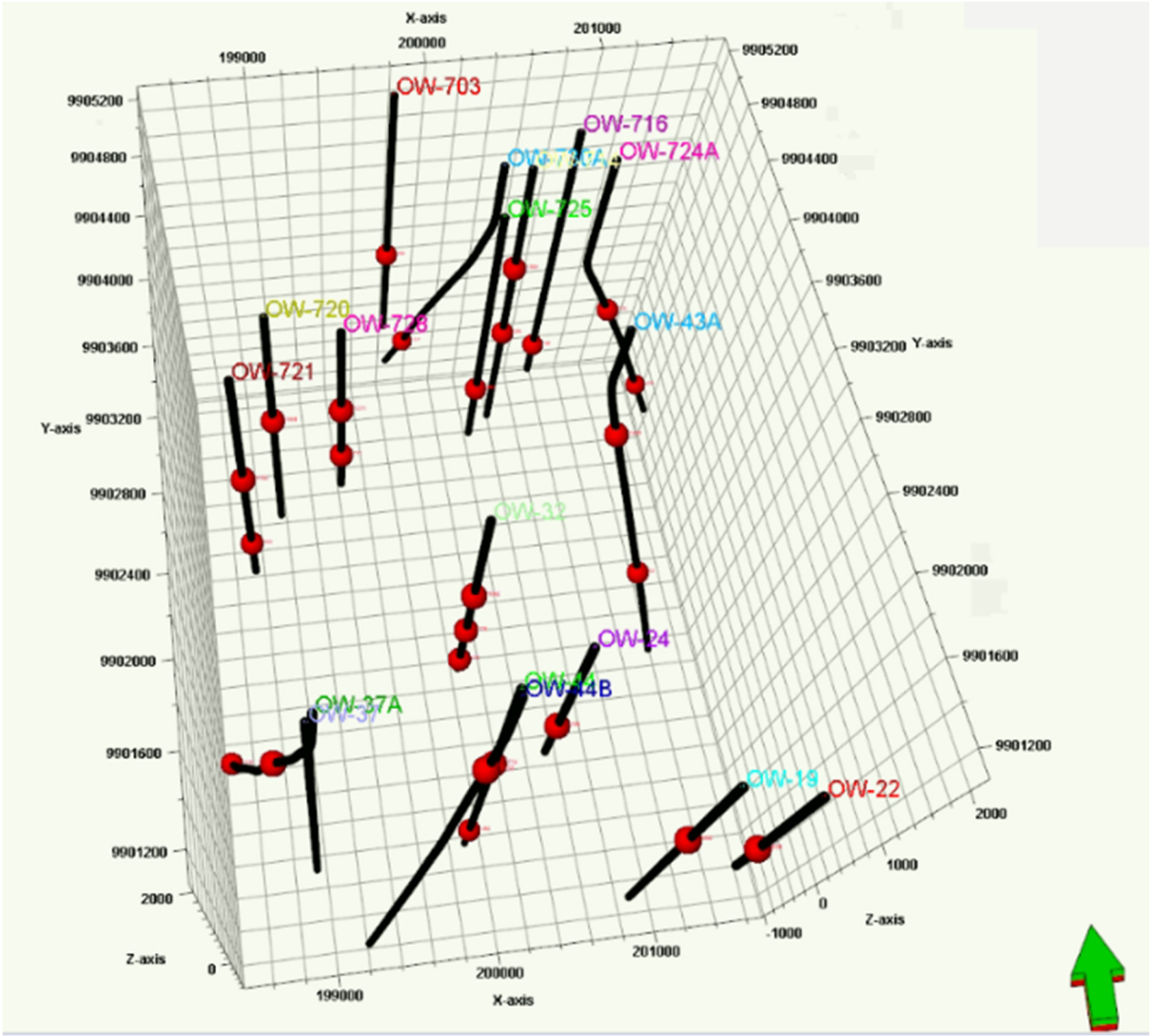

FIGURE 11: Location of re-injection well OW-703 in relation to production wells

3.4 Sampling of production wells

Fluid samples were collected daily from 32 wells (Table 6) spread across the OEPF and ONEPF during the first month after tracer injection into OW-703. The sampling frequency was subsequently reduced gradually down to twice a week during the last month of sampling. This was to ensure that possible fast tracer arrivals in boreholes were well captured during the sampling period. Due to tracer dispersion over time and distance, the sampling frequency was reduced in the later months.

TABLE 6: Characteristics of the sampled production wells

Well No	Mass flow (kg/s)	Well Total Depth (m)	Production Casing Depth (m)	Distances to main feed zones (m) from OW-703
16	22.2	901	497	4200
19	4.4	1049	489	4068
22	1.5	1234	545	4241
24	0.8	2993	958	3288
26	13.7	1406	545	3060
27+31+33	8.7	1348/1620/1607	537/558/545	3500
32	11.7	1600	547	2587
37A	10.8	2267	498	3168/3435
37B	1.7	3000	750	4250
43	1.5	3000	751	2000
43A	4.6	3001	742	2062/2508
44	7.6	2800	1190	3212
44B	5.8	2882	956	3532
701	6.8	1101	636	1100
720+728	25.9	2006/2015	690/651	1638/1558
709	3.9	2504	890	1900
712	4.3	2590	793	1280
714	26.1	1744	717	928
716	14.4	3000	809	1051
719	35.5	2007	886	1370
721	10.2	2099	702	2080
724A	33.3	3000	757	1462/1818
725	28.9	1898	632	1070
726	8.3	1801	654	1080
730A	6.5	3000	1203	143
730B	9.4	2877	958	440
732	18.6	3000	801	1200
732A	32.5	3010	1206	1300

In the case of the online wells, liquid samples were collected from the lowest level of the sampling line by opening the valves in the two-phase lines. For wells being discharge-tested, samples were collected from the weir box.

Once the valve opening had been adjusted for safe sample collection, the sample was left to drain for a couple of minutes before using the liquid to rinse out the sampling bottle three times prior to sample collection. This is undertaken to avoid any cross-contamination of the samples. The liquid phase samples were untreated and were collected in airtight glass bottles and once filled they were clearly labelled with the well numbers and the cap completely tightened. During sampling, the well head pressure was recorded. The samples were analysed for pH, temperature, conductivity, sodium fluorescein, and chloride concentrations.

3.5 Tracer recovery and modelling

All collected samples were analysed by KenGen using their equipment and techniques. A total of 9 of the 32 (28%) production wells monitored for the 23 weeks (almost six months) period showed significant tracer recovery of the injected sodium fluorescein tracer, confirming the influence of the re-injection water on the field. This is summarized in Table 7, tabulated in detail in Table 8 and graphically presented in Figure 12 below. In the figure, the production wells that show a positive response to the injected tracer are indicated. Both the measured and modelled recovered mass were estimated using the TRINV software.

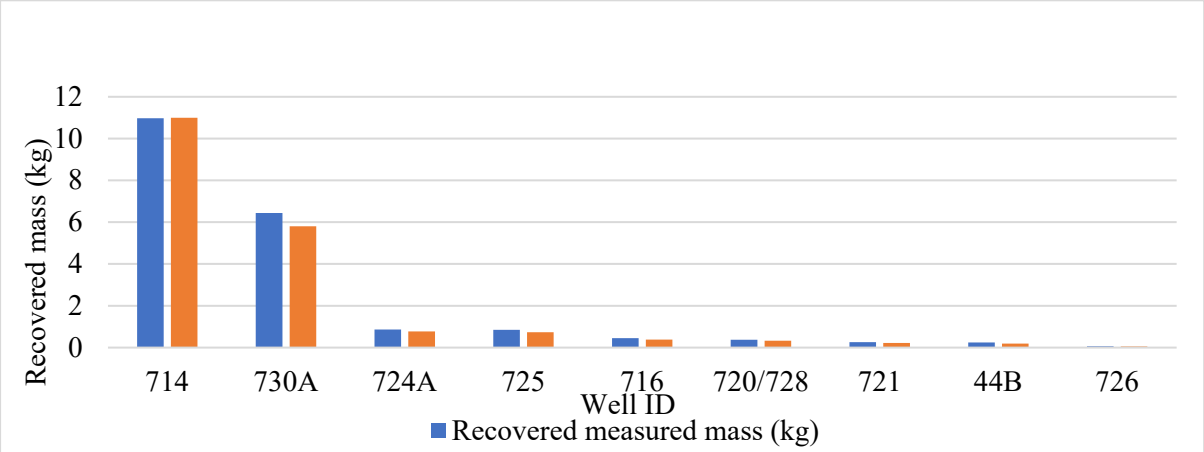

FIGURE 12: Positive sodium fluorescein tracer recoveries in the ONEPF and OEPF, Olkaria, after injection into well OW-703

TABLE 7: Summary of the Olkaria wells that showed sodium fluorescein tracer recovery

Injection Well (Tracer)	**Production wells with positive tracer response**	**Remarks**
OW-703	OW-730A and OW-714	ONEPF, relatively good recovery
OW-703	OW-724A, OW-725, OW-716, OW-721, OW-720/728 and OW-726	ONEPF, minimal recovery
OW-703	OW-44B	OEPF, minimal recovery

TABLE 8: Measured and modelled (TRINV) tracer recovery through Olkaria wells after 550 kg of sodium fluorescein tracer was injected into well OW-703

Well No.	Measured mass recovery (kg)	Measured tracer recovery (%)	Modelled mass recovery (kg)	Modelled tracer recovery (%)
714	10.97	2.00	11.00	2.00
730A	6.44	1.17	5.80	1.05
724A	0.86	0.16	0.77	0.14
725	0.85	0.15	0.73	0.13
716	0.45	0.08	0.38	0.07
720/728	0.37	0.07	0.33	0.06
721	0.26	0.05	0.22	0.04
44B	0.24	0.04	0.19	0.03
726	0.06	0.01	0.05	0.01
TOTAL	20.50	3.73	19.47	3.53

By observing and analysing the tracer recovery data, some basic aspects of the process can be observed. These include (1) the tracer breakthrough-time which depends on the maximum fluid velocity, (2) the time of the concentration maximum which reflects the average fluid velocity, (3) the width of the tracer pulse which reflects the flow-path dispersion, and (4) the tracer recovery (mass or percentage, see Table 8) as a function of time (Axelsson et al., 2005).

Modelling plays a key role in understanding the nature and estimating the properties of geothermal systems. It is a powerful tool for predicting their response to future production and consequently to estimate their production capacity. Modelling is also an indispensable part of successful geothermal resource management during utilization (Axelsson, 2013c).

3.6 ONEPF response to exploitation and reinjection

As part of KenGen´s reservoir management, the output of production wells is monitored bi-annually (for January-June and July-December, respectively) and is mainly done to help observe important changes that could be taking place in the reservoir. The properties monitored include the well-head pressure, temperature, enthalpy, mass output and physical characteristics like cyclicity. According to Mariaria (2012), such changes could be the result of reservoir boiling, over-exploitation, entry of cold water into the reservoir, wellbore scaling or direct re-injection returns in the reservoir. As part of the geothermal resources management, it is important to understand a geothermal system well and subsequently monitor its response to long-term utilization (Monterrosa and Axelsson, 2013; Axelsson, 2008). Careful monitoring techniques help to map out thermodynamic and chemical changes before they cause adverse effects in the reservoir. It also provides important data on the nature and characteristics of geothermal systems, information which is indispensable for the development of geothermal conceptual and numerical models (Axelsson, 2013b). Figures 13 to 17 shows changes in the characteristics of the main wells involved in this study over time.

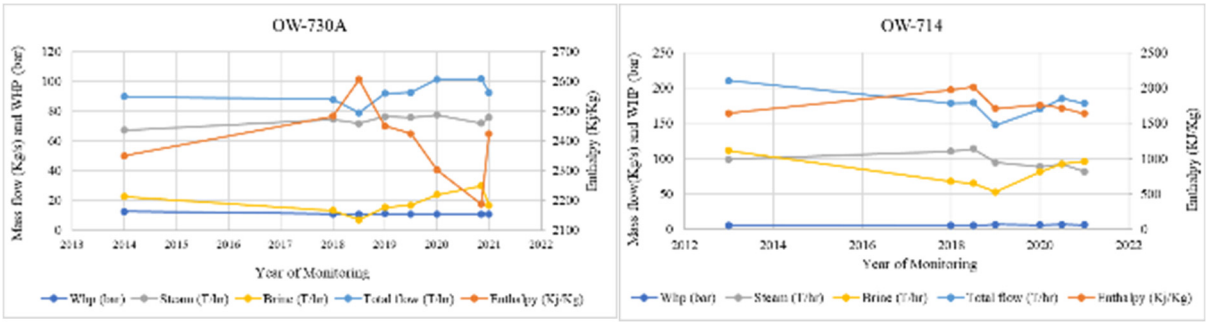

FIGURE 13: Well parameters of wells OW-730A and OW-714 over time

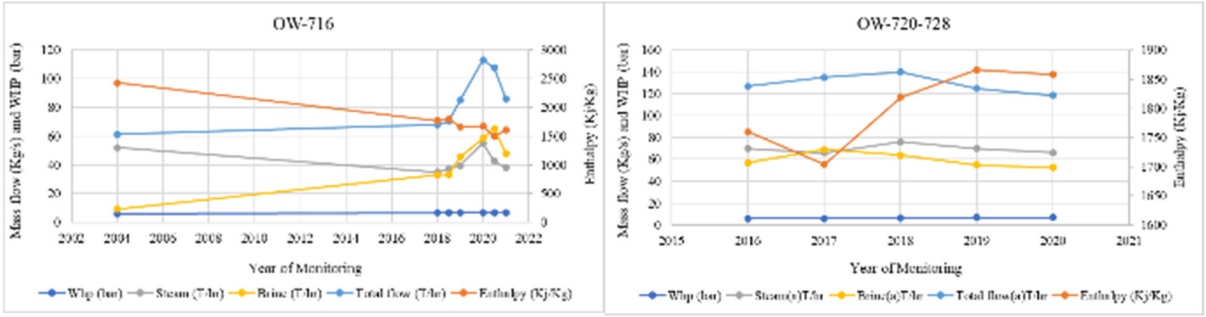

FIGURE 14: Well parameters of wells OW-716 and OW-720 + OW-728 over time

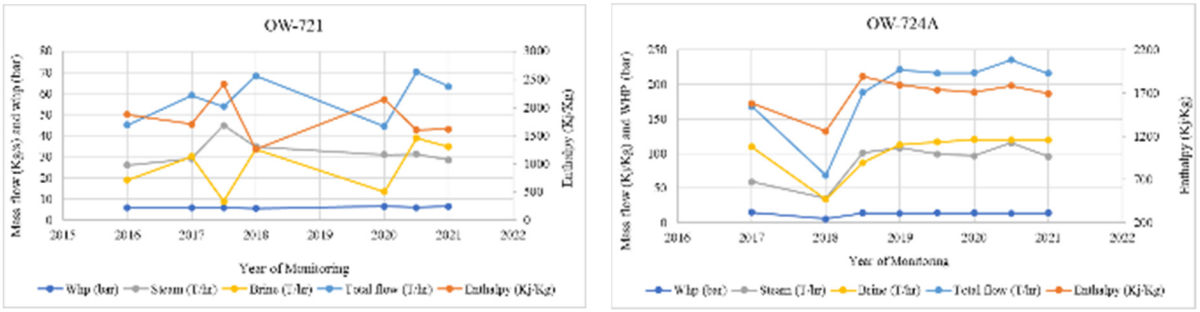

FIGURE 15: Well parameters of wells OW-721 and OW-724A over time

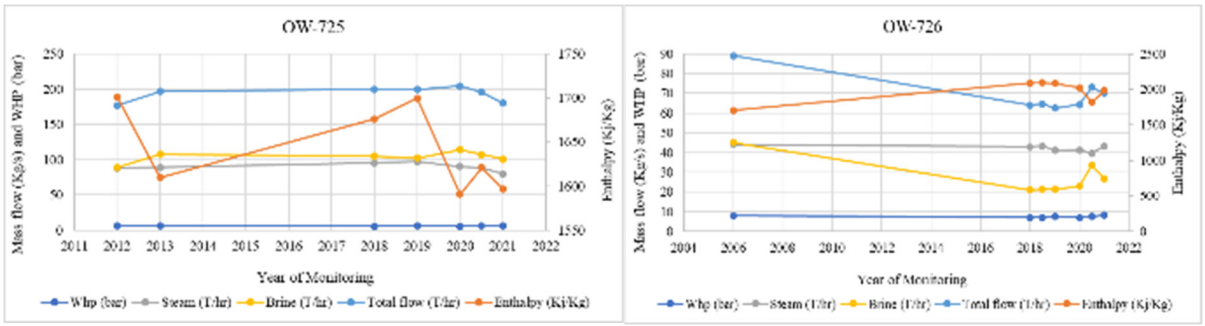

FIGURE 16: Well parameters of wells OW-725 and OW-726 over time

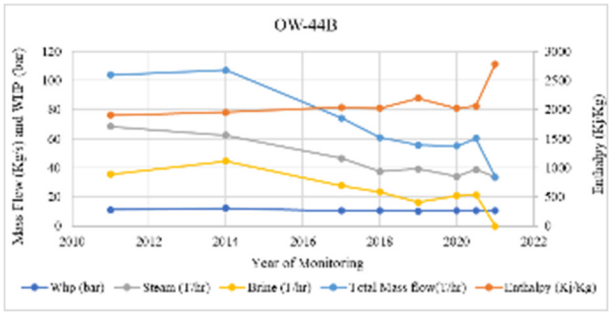

FIGURE 17: Well parameters of well OW-44B over time

In terms of enthalpy, the field has remained relatively stable with a slight change southwest of well OW-703. Figures 18-20 show the measured enthalpy of ONEPF wells in 2017, 2019 and 2021, respectively.

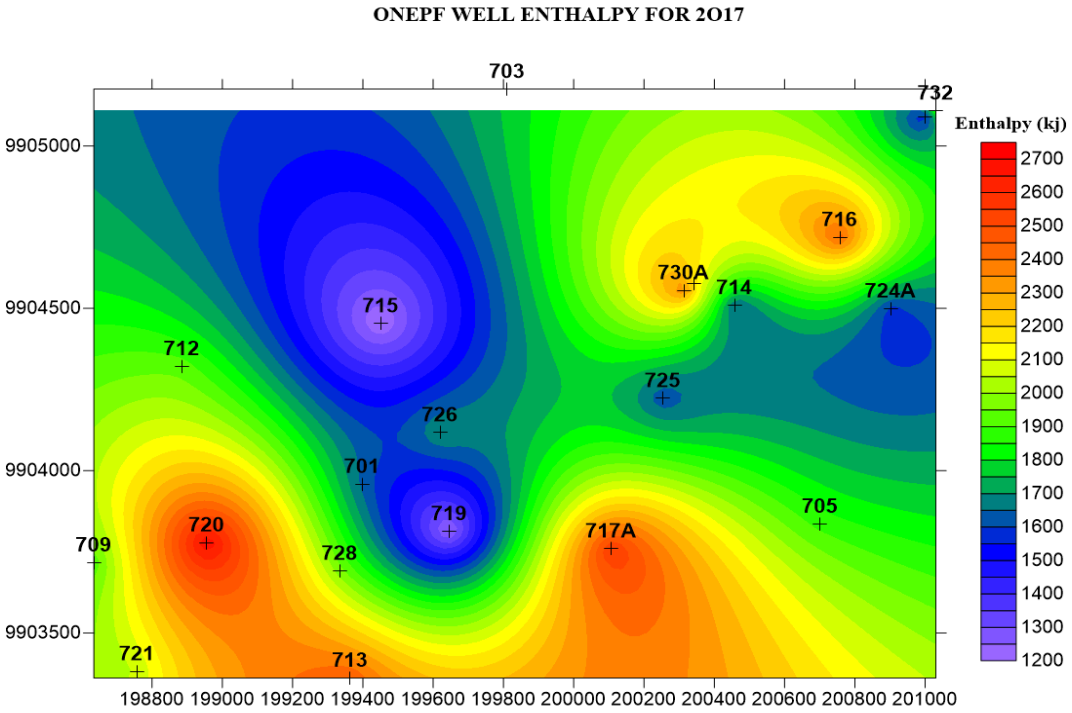

FIGURE 18: Enthalpy distribution for ONEPF wells in 2017

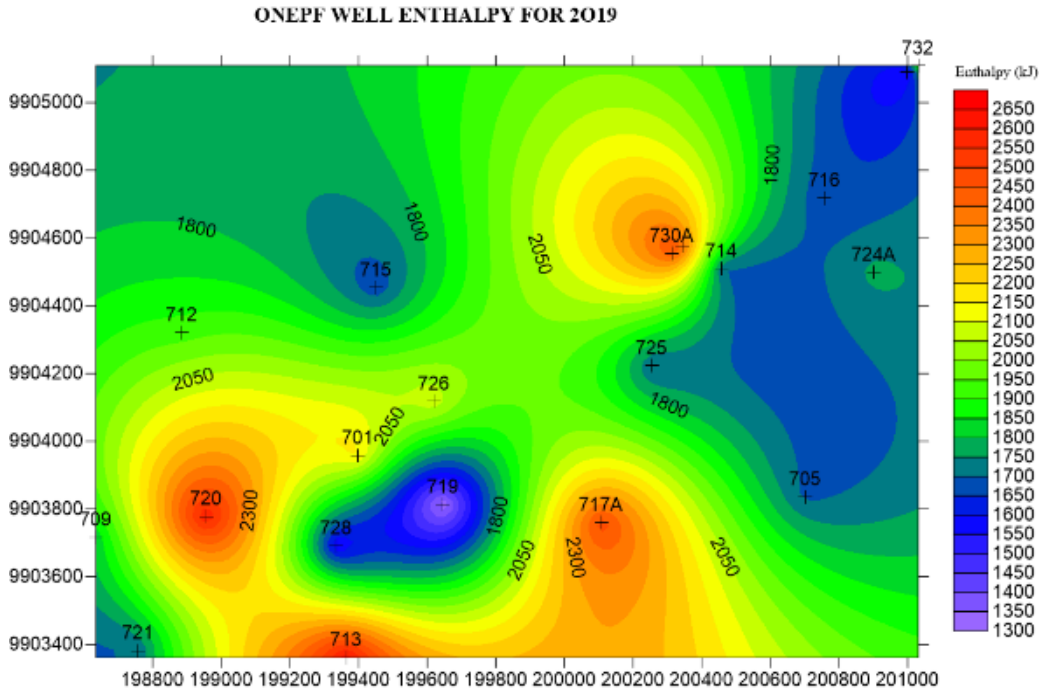

FIGURE 19: Enthalpy distribution in for ONEPF wells in 2019

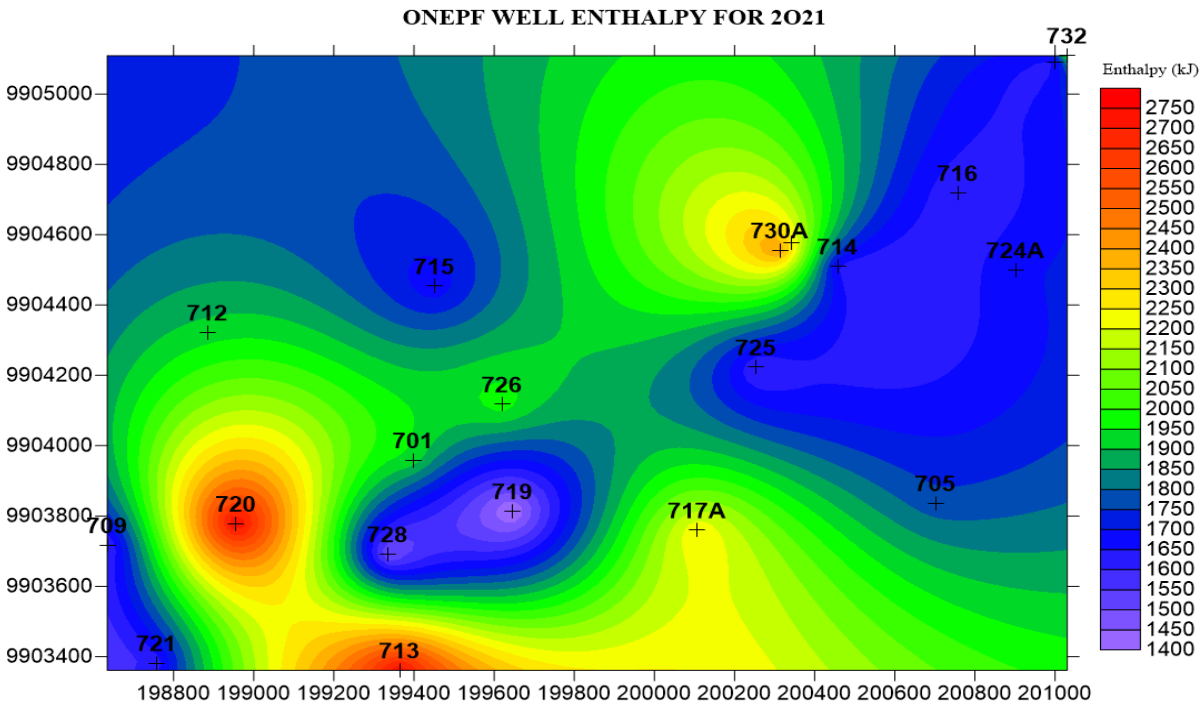

FIGURE 20: Enthalpy distribution for ONEPF wells in 2021

4. ANALYSIS OF TRACER RECOVERY DATA

4.1 Modelled tracer recovery

The data obtained from the sample analysis, for wells showing significant recovery during the tracer test, were fed into the TRINV software package for data processing and tracer test analysis resulting in complete tracer breakthrough curve simulation, inversion of tracer test data and cooling predictions for the production wells. Figures 21 to 29 show the modelled tracer recovery for the 9 wells that showed significant recovery.

Considerable scatter was noted in the data, and this is attributed to the following possible influences: The cyclic nature of some wells in the field, possible contamination of the brine with steam condensate, possible contamination by personnel carrying out the exercise, and limited analysing accuracy. The generally low tracer returns in this test may, furthermore, be because of tracer decay.

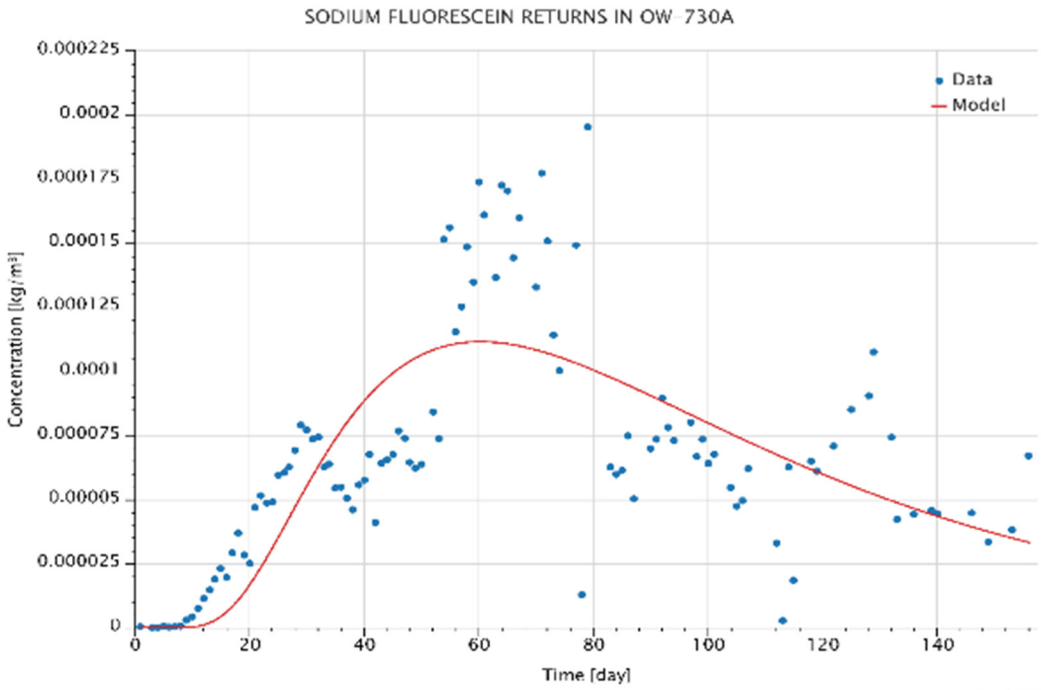

FIGURE 21: Observed and modelled tracer recovery through Olkaria well OW-730A

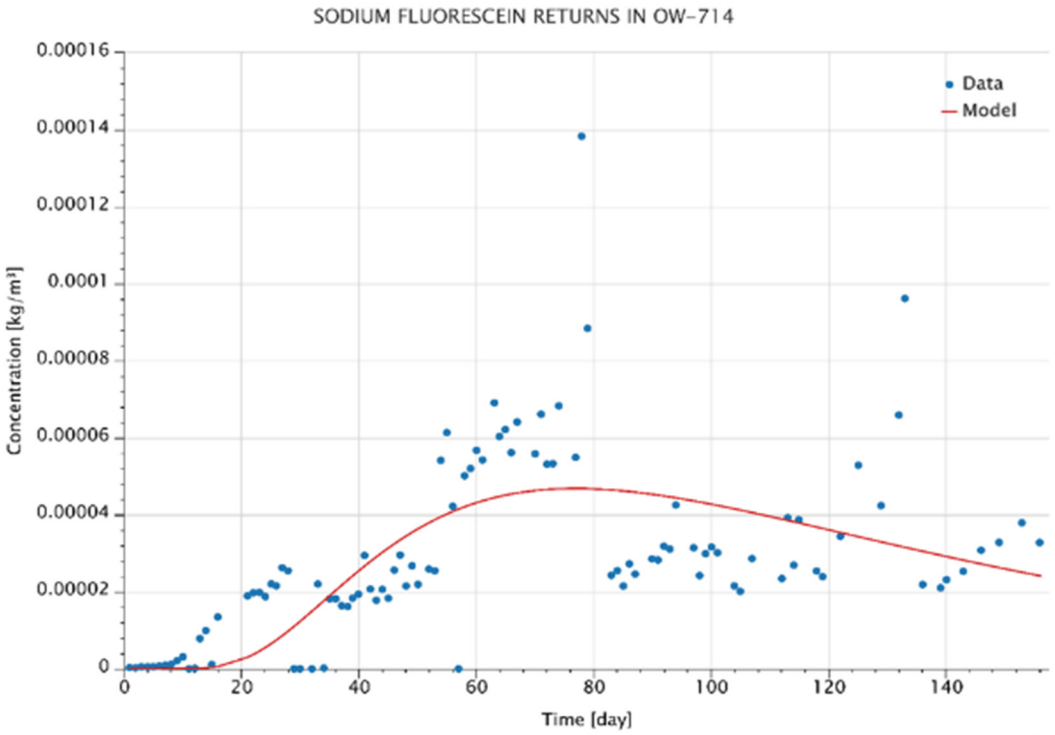

FIGURE 22: Observed and modelled tracer recovery through Olkaria well OW-714

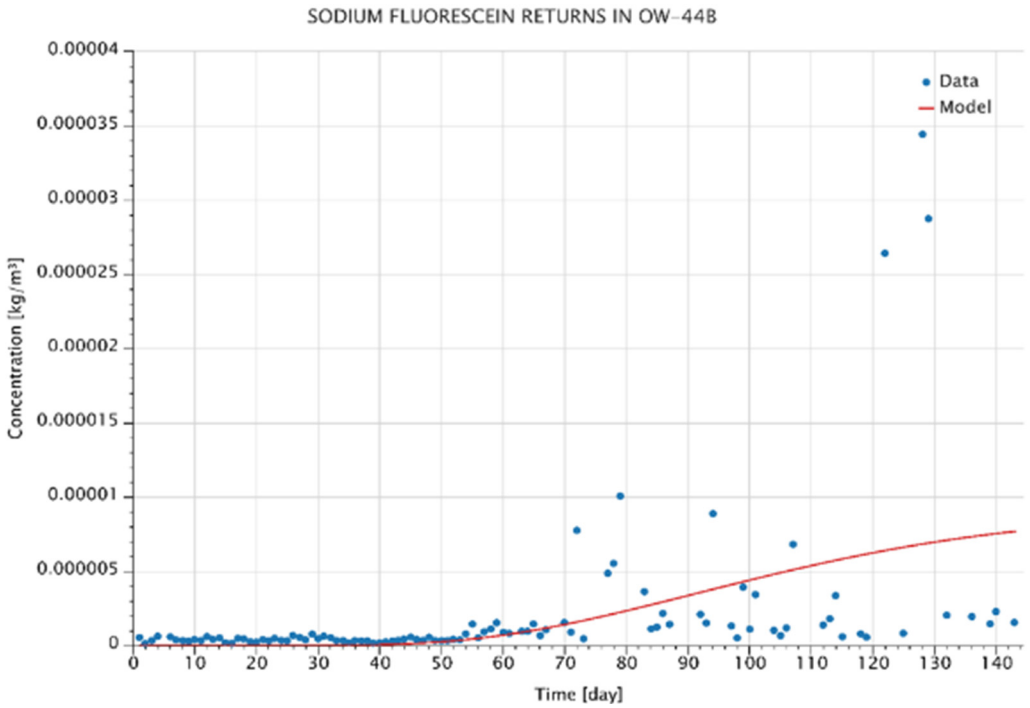

FIGURE 23: Observed and modelled tracer recovery through Olkaria well OW-44B

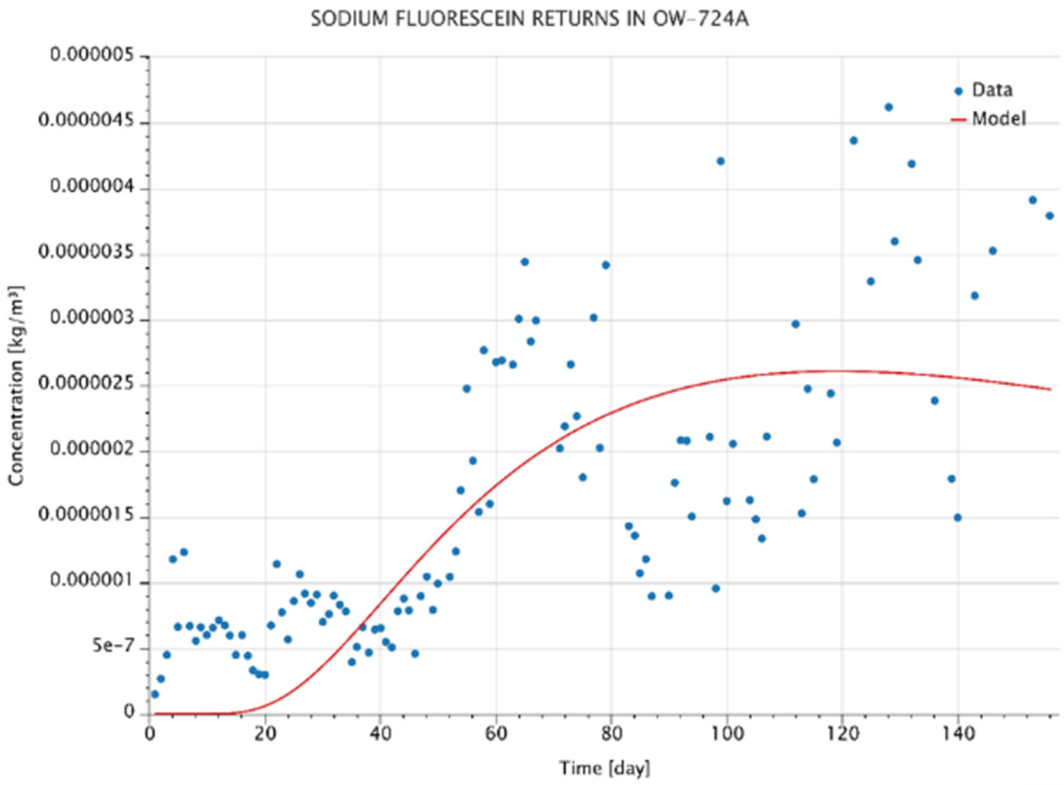

FIGURE 24: Observed and modelled tracer recovery through Olkaria well OW-724A

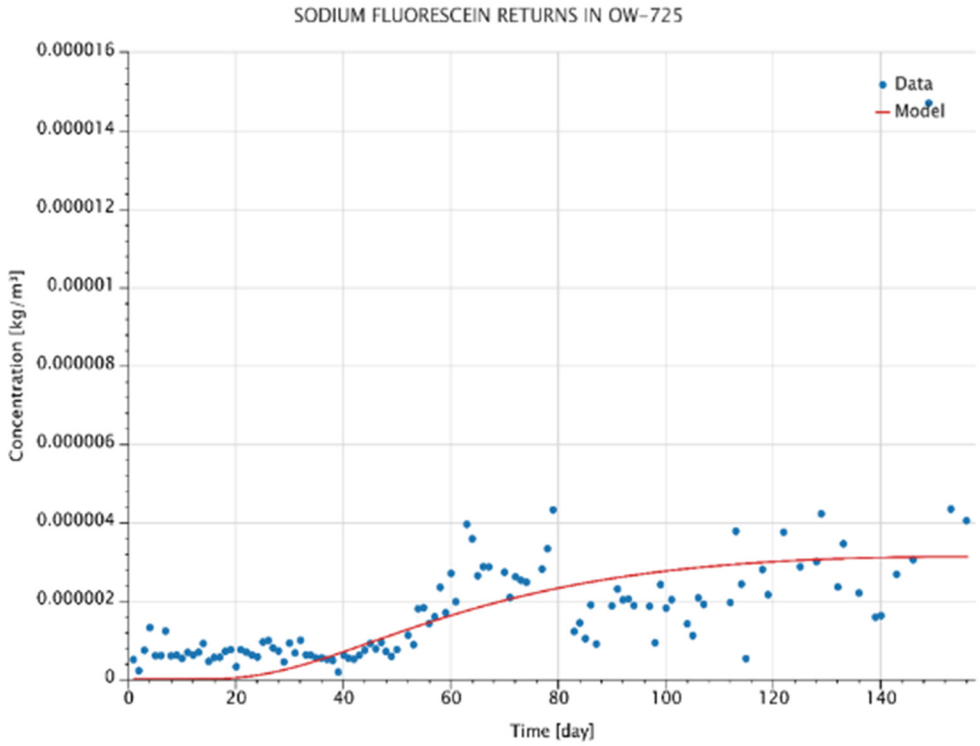

FIGURE 25: Observed and modelled tracer recovery through Olkaria well OW-725

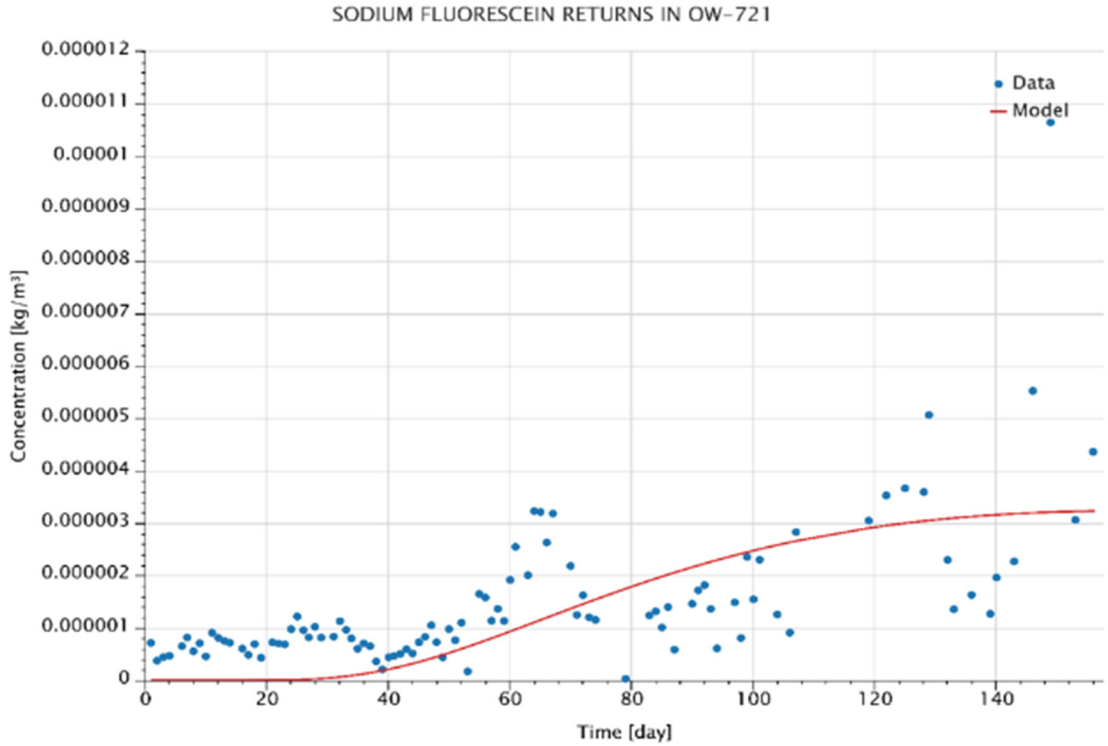

FIGURE 26: Observed and modelled tracer recovery through Olkaria well OW-721

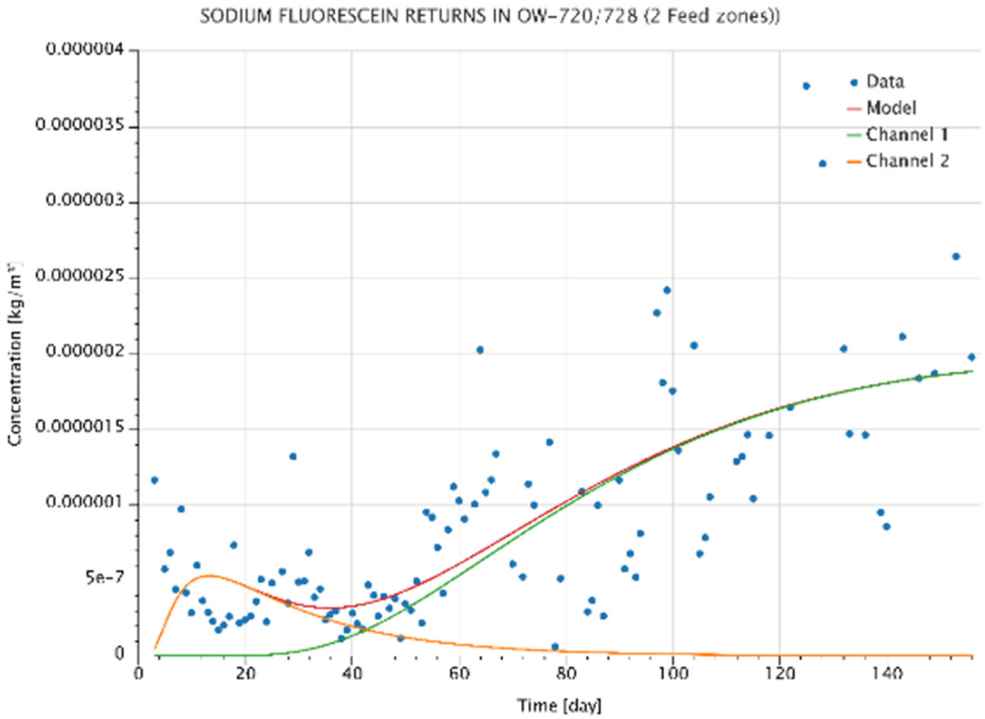

FIGURE 27: Observed and modelled tracer recovery through Olkaria wells OW-720+728

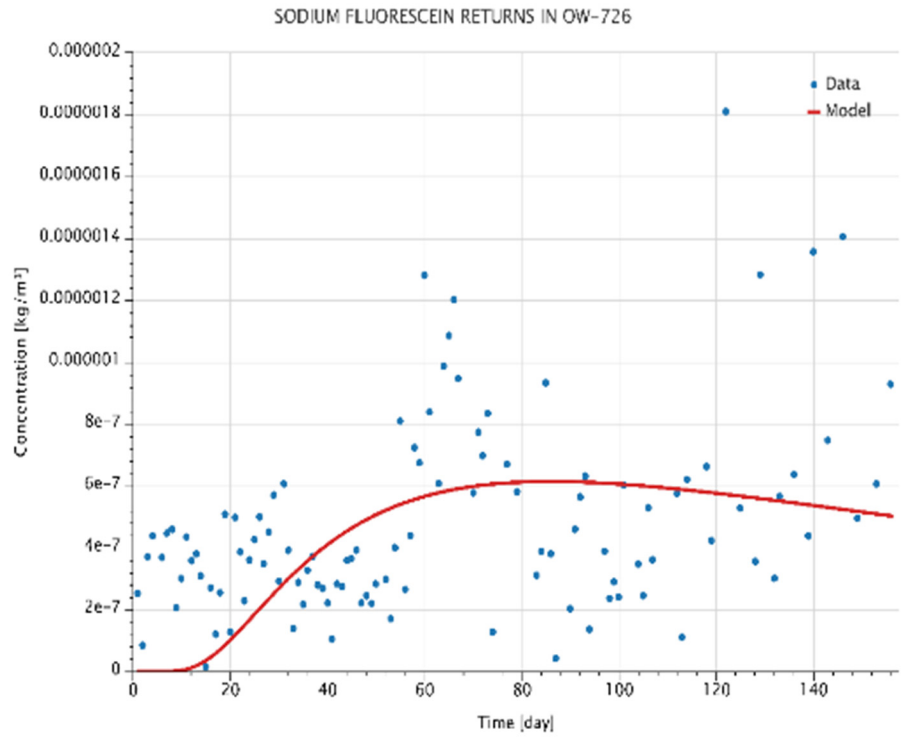

FIGURE 28: Observed and modelled tracer recovery through Olkaria well OW-726

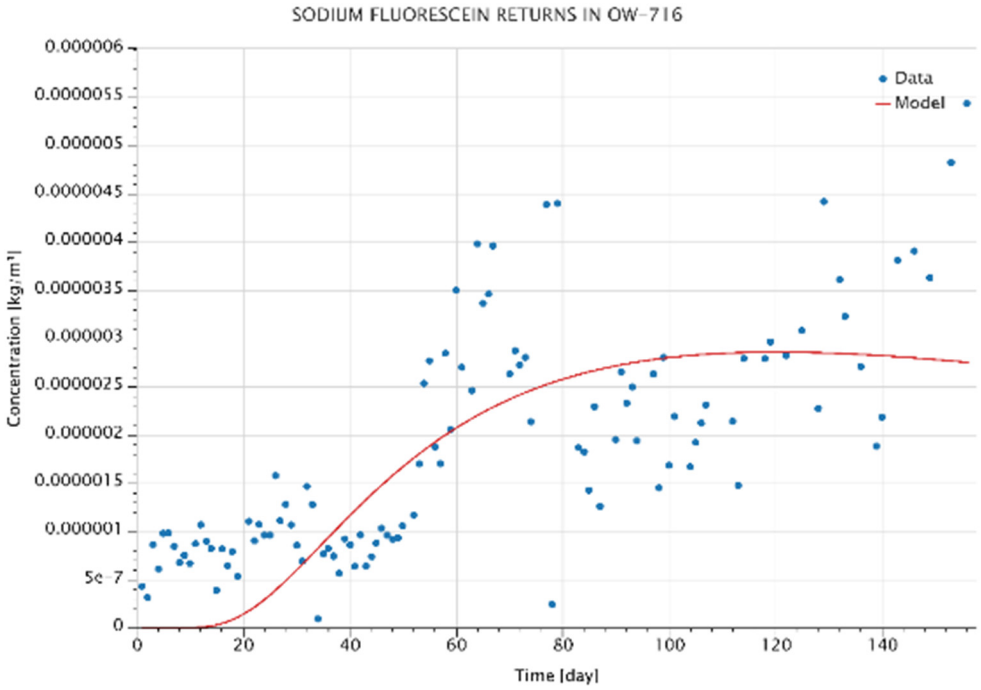

FIGURE 29: Observed and modelled tracer recovery in Olkaria well OW-716

4.2 Possible tracer-decay due to temperature

The tracer used in this test was sodium fluorescein. Sodium fluorescein has been studied experimentally at temperatures ranging from 150 to 300°C and it has been noted that it degrades thermally at higher temperatures. Its half-life has been found to be 150 days at 220°C and 37 days at 250°C. Therefore, it is recommended for use in geothermal tracer testing for reservoirs with temperatures below 210°C as it decays by less than 10% in one month at these temperatures (Adams and Davis, 1991).

At a constant pH, fluorescein decays according to a first order rate law given by:

$$C(t) = C_0 e^{-kt} \quad (3)$$

where C(t) = Concentration of fluorescein after heating (mg/l);
Co = Initial concentration (mg/l);
t = Time (s); and
k = A decay parameter (s^{-1}).

The temperature dependent decay parameter k can be described by an Arrhenius relationship as (Rose et al., 2000):

$$k = Ae^{(-Ea/RT)} \quad (4)$$

where E_a = Energy of activation (J/mol);
A = Pre-exponential constant (s^{-1});
T = Sample absolute temperature (K); and
R = Universal gas constant = 8.31 J/mol K

The activation energy E_a and the natural logarithm (ln) of the pre-exponential constant A have been estimated as 143,300 (±6,620) J/mol and 18.25 (±1.44) s^{-1}, respectively (Adam and Davis, 1991).

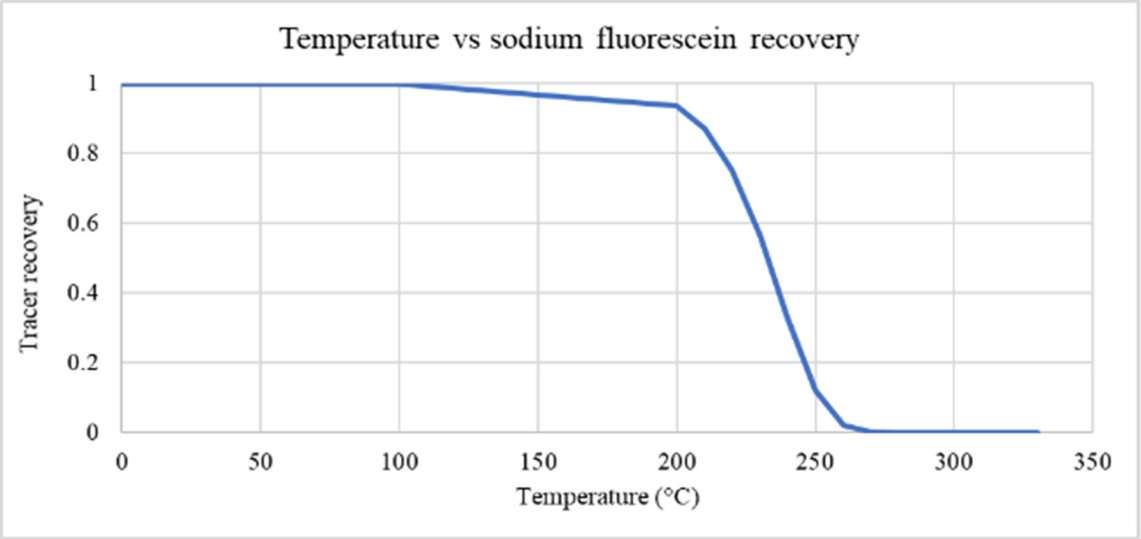

FIGURE 30: Estimated tracer recovery in the study area, taking thermal decay of sodium fluorescein into account, presented as a function of average reservoir temperature

From the pressure and temperature logs of wells OW-714, OW-730A and OW-724A, the formation temperature has been estimated to be 285°C. This is in line with other wells in the geothermal field. All the wells drilled in the ONEPF have formation temperatures of over 240°C with most actually having temperatures higher than 310°C (Ambusso and Ouma, 1991). Considering that the hot brine injected into re-injection well OW-703 is at an average temperature of 150°C, the assumption is made that it will take some time before the brine is heated to the formation temperature (285°C). Explicitly solving for the real temperature distribution between the re-injection well and the production wells is a complex task, thus a temperature of 230°C was used as an estimate of the average temperature in the flow channels between the re-injection well and wells OW-714, 730A and 724A. The peak in tracer return for well OW-730A was seen after 60 days, which is used here as an estimate of the average residence-time of the reinjected water. Figure 30 shows the estimated tracer decay, using equations (3) and (4), with the residence-time of 60 days. At 230°C, sodium fluorescein decays by almost 60% after 60 days. The tracer recovery goes down exponentially with increasing temperature, going to zero at around 270°C.

Due to the presence of tracer in the production wells studied here, despite relatively high decay rate, it can be conclusively said that there are hydrological connections between the re-injection well and the production wells highlighted above. However, for cooling estimates, it is important to factor in the tracer decay because some of it could have thermally decayed over time due to high reservoir temperatures. Therefore, the tracer models presented in chapter 4.1 give an optimistic cooling prediction though the pessimistic estimations in each of Figure 31-33, represent a more realistic situation in terms of cooling predictions, as they indirectly make up for the effect of thermal decay of sodium fluorescein.

4.3 Cooling predictions

During this tracer test, it was noted that well OW-703 received 178 kg/s of hot brine from the neighbouring wells as tabulated earlier in Table 5. Cooling predictions were calculated using the TRINV software for the three wells that showed the strongest connections to the re-injection well OW-703, i.e. wells OW-730A, OW-724A and OW-714. All these wells have formation temperatures of about 285°C with the temperature of the re-injected brine being 150°C. The modelling results are summarized in Table 9 below.

TABLE 9: Cooling prediction results for Olkaria wells OW-730A, 724A and OW-714.

	Reservoir temperature (°C) after 10-year reinjection with different flow-channel height-to-width ratios		
Well ID	Optimistic ratio of 100:1	Average ratio of 10:1	Pessimistic ratio of 1:1
OW-730A	270	250	243
OW-724A	285	285	284
OW-714	284	272	265

The minimum distance from the re-injection well to the feed zones of these wells are 143 m, 1462 m and 928 m, respectively. The cooling predictions for the wells are shown in Figures 31-33. This was modelled based on continuous field utilization for 10 years. This is a relatively optimistic approach as some tracers could have thermally decayed in the reservoir during the monitoring period because of high reservoir temperatures. Each of the wells was modelled based on a varying height to width ratio of the main flow-channel connecting it with the reinjection well. The pessimistic case is when the height of the reservoir was assumed to be equal to its width (1:1), the average case is with a height that is ten times the width (10:1) and in the most optimistic approach the flow-channel´s height is assumed to be 100 times its width, or 100:1 (long and narrow fracture-zone flow-channel).

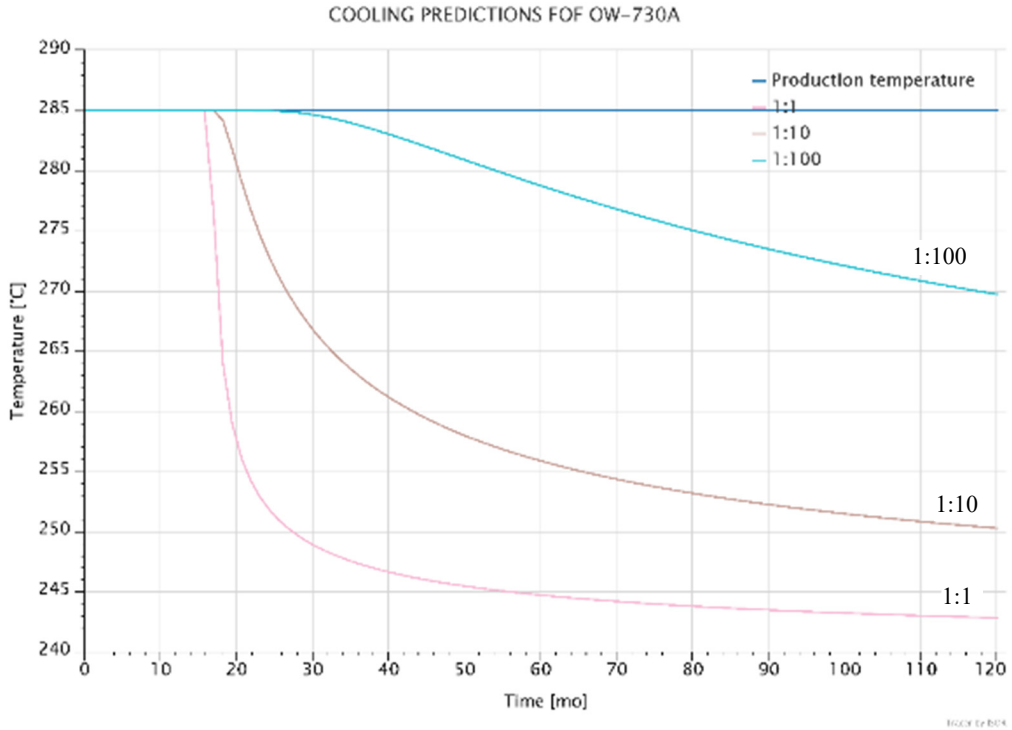

FIGURE 31: Cooling predictions for well OW-730A for different flow-channel width-to-height ratios

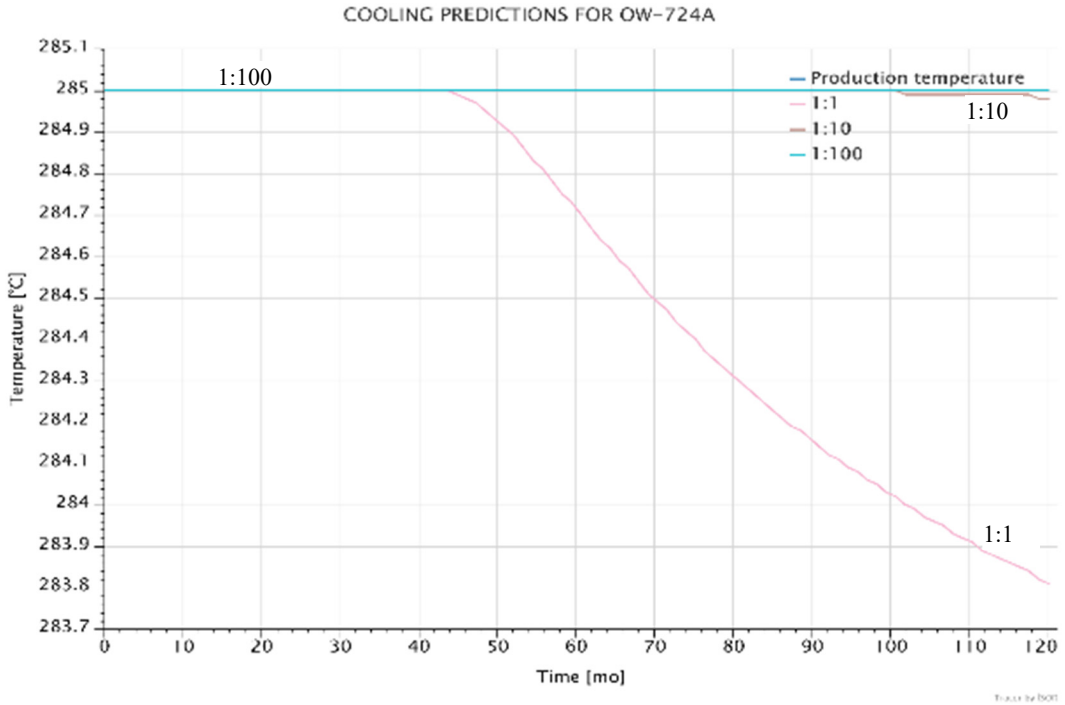

FIGURE 32: Cooling predictions for well OW-724A for different flow-channel width-to-height ratios

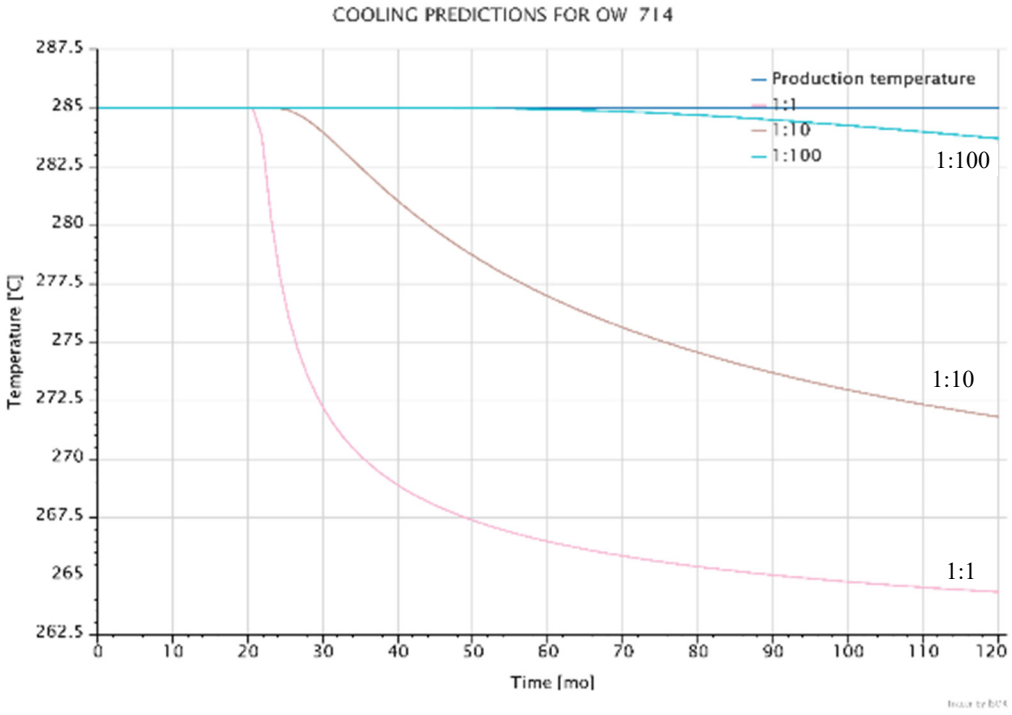

FIGURE 33: Cooling predictions for well OW-714 for different flow-channel width-to-height ratios

In the cooling predictions for OW-730A, it is noted that when the width to height ratio is 1:1, the reservoir temperature starts to drop drastically from 285°C in the 16th month to 257°C in the 20th month. Thereafter, the temperature remains almost stable as it drops from 257°C to 243°C in 100 months. For the 1:10 ratio, the formation temperature drops from 285°C in the 18th month to 257°C in the 120th

month while for 1:100, the temperature drops from 285°C in the 28th month to 270°C in the 120th month (Figure 31).

For OW-724A, the volume of the re-injected brine recovered is lower than it is in OW-730A. For the pessimistic scenario, where the width to height ratio is 1:1, the temperature will start to drop in the 44th month from a formation temperature of 285°C to just 283.8°C in the 120th month. For the 1:10 and 1:100 ratios, the well would not be affected by this re-injection for the whole prediction period of 10 years (Figure 32).

For OW-714, at a reservoir width to height ratio of 1:1, the temperature drops by about 20°C, from a formation temperature of 285°C to 264.5°C from the 20th month to the 120th month. For the 1:10 ratio, the fluid temperatures drops from 285°C to 271.5°C from the 25th month to the 120th month, while for the 1:100 ratio, it drops from 285°C to around 284°C from the 60th month to the 120th month. This can be attributed to the relatively high tracer recovery in the well (Figure 33).

5. DISCUSSION

KenGen has embraced tracer testing as part of its reservoir management strategies. This has been done consistently for the last 18 years. ONEPF is a crucial part of the Greater OVC and KenGen has drilled over 10 re-injection wells in that area. The sub-field hosts the 105 MW_e Olkaria II power plant, the KenGen Spa and supplies steam to the 140 MW_e Olkaria IAU power plant. The wells in the field must be maintained for continuous supply of high temperature steam to these power plants. Re-injection, therefore, is one way of maintaining the wells in the field through maintaining reservoir pressure. Tracer test recoveries from other wells show that the brine injected into OW-703 finds its way into some of them. Fluids travel in the subsurface either though structures (faults, fractures, lithological boundaries, etc.) or through rock pores. Olkaria has several geological structures and it is evident that the fluid flows and thermal energy conveyance in N-S direction is influenced by these structures. Figure 34 shows the main faults and structures in OVC. The adaptive reservoir management approach used in Olkaria ensures that the tracer test results influence the reservoir management strategy while managing the requirements of an operating field. Presently, KenGen has several re-injection wells (Table 3) across the ONEPF with different well connections between them and the production wells. This ensures that most, if not all the wells, are hydrologically supported over time by the re-injection strategy. Currently, OW-703 is supposed to be used intermittently with OW-718 and future re-injection well locations/ sites should consider the results of previous tracer tests.

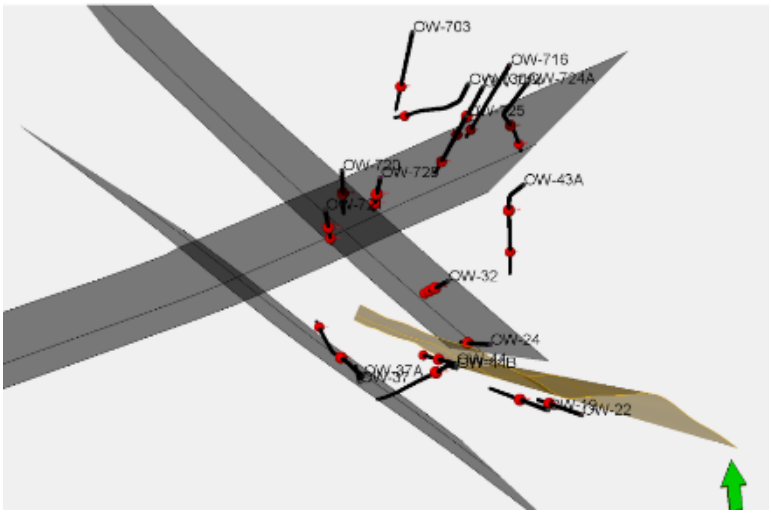

FIGURE 34: Location of fractures, faults, and wells in OVC

KenGen undertakes periodic production monitoring and downhole pressure and temperature logs to assist in detecting early signs of thermal breakthrough in the field. Only a few of the monitored production wells in the field showed substantial signs of tracer recovery. Those that showed some form of tracer recovery also showed direct changes in mass flows (mostly brine) and indirect changes in enthalpy. As brine injection takes place in the field, the wells that have connections with the re-injection well show a slight increase in mass flows but a slight decrease in enthalpy.

In terms of cooling predictions, it should be noted that the ONEP is a hot-temperature area with an up-flow zone, thus the field is heating up over time. This is observed by elevated values of CO_2 and platy calcite in the field (Kandie, 2017; Wamalwa et al., 2016). Re-injection of brine in the field seems to have somehow delayed the boiling in the field otherwise expected due to pressure decline. The two wells, OW-730A and OW-714, that showed significant tracer recoveries are close to each other on the surface and less than a kilometre south of the re-injection well on surface. However, at depth, OW-714 is less than 150 m away from the re-injection well. Re-injection of hot brine into the system does not seem to cause any fast thermal breakdown. The cooling predictions for both OW-730A and OW-714 indicate that the reservoir temperatures will remain unaffected and at equilibrium for 16-20 months and 30-70 months for the pessimistic and optimistic models, respectively. And even when the temperatures finally go down after 10 years, they are still at a minimum of around 243 and 264°C for wells OW-730A and OW-714, respectively. The third well, OW-724A, is about 1.5 km away from the reinjection well OW-703 and according to the cooling predictions, the well would still be at equilibrium even after 10 years of brine injection into well OW-703.

The prediction results should be considered optimistic as the tracer used, sodium fluorescein, is known to thermally decay when exposed to higher temperatures for a long period. The recovered tracer was just under 10% of the reinjected tracer, thus, a significant amount of the tracer could have been 'lost' as result of thermal decay. The Olkaria formation temperature is known to be over 240°C and sodium fluorescein is known to decay at temperatures higher than 230°C. Therefore, the cooling predictions calculated for the 3 wells can be considered optimistic. The pessimistic graph in each case can perhaps be assumed to be close to the realistic situation in the geothermal field, because of the thermal decay of sodium fluorescein.

6. CONCLUSIONS AND RECOMMENDATIONS

The main goal of this study was to assess and discuss how re-injection has been managed in the Olkaria geothermal field in Kenya, with specific emphasis on the Olkaria Northeast Production Field (ONEPF), and evaluate its role in resource management especially regarding brine re-injection into well OW-703. This was done by monitoring of wells in both the ONEPF and the OEPF prior to and after injection of the chemical tracer sodium fluorescein. The results were then modelled using the tracer inversion software TRINV where modelled and measured tracer recovery values were matched. The software was also used to predict cooling for the 3 wells that showed significant connections to OW-703. On basis of the results of this test, permeability characteristics and geothermal flow paths in the ONEPF can be modelled and used to improve the conceptual and numerical models of the resource.

Data obtained from the routine biannual tracer flow test (TFT) in the field for the past 5 years was evaluated and graphs and contour maps plotted (Figures 13-20) based on them. These figures give an overview of how the field has been responding to geothermal utilization in terms of wellhead pressures, mass flows (both steam and brine) and enthalpies. Therefore, based on the above results, after applying the methods described earlier to data from the Olkaria geothermal system, the following conclusions can be drawn:

- The results of the sodium fluorescein tracer test involving injection well OW-703 provided useful insights into the nature of subsurface permeability in the OEPF and ONEPF by confirming that the faults and fractures play a major role in fluid flow in the geothermal field. It was noted that there are hydrological connections between the injection well OW-703 and some of the production wells. These production wells include Olkaria wells OW-730A, OW-714, OW-44B, OW-724A, OW-725 and OW-721. This information is crucial as it will be utilized in the management of key reservoir risks in the field, especially the ones associated with unfavourable well connections and thermal breakthroughs. Wells OW-714 and OW-730A showed the highest tracer recoveries.

- Pessimistic cooling predictions showed that with continuous re-injection of 178 kg/s of hot brine into well OW-703 for 10 years, the reservoir temperatures would decrease from 285°C to around 243°C and 264°C for OW-730A and OW-714, respectively, assuming low height to width flow channel ratios. For a higher ratio the cooling would be considerably less. According to this model, well OW-724 will not show any signs of cooling because of this re-injection in the next 10 years.

- The overall rate of tracer recovery was very low, approximately 20 kg (about 4% of the injected 550 kg), and the process modelling results indicate that the sodium fluorescein compounds used in the ONEPF reservoir may not have been totally stable during the tracer test period. Sodium fluorescein is known to thermally decay at a relatively fast rate at high temperatures (over 230°C). Therefore, the cooling predictions may constitute an underestimate.

- Considering that re-injection well OW-703 is usually used intermittently with OW-718 and the brine injected has a temperature of 150°C, this prolongs the time it will take for thermal breakthrough in the field.

- It is, therefore, recommended that the use of well OW-703 as an intermittent re-injection well be continued. This is also supported by the enthalpy and mass flows measured in the field.

- The routine biannual TFT measurements should be done as scheduled for all the production wells in the field to confirm the reservoir behaviour regarding geothermal utilization in the area.

- More appropriate tracers with known thermal decay kinetics e.g., the NDS family (Naphthalene Disulfonate) should be used in the higher temperature Olkaria geothermal field for both qualitative and quantitative data analysis.

- With the increased drilling activity in the Olkaria geothermal field it is recommended that a tracer test will be redone for re-injection well OW-708 to assess the well connections to other wells within the ONEPF vicinity.

7. ACKNOWLEDGEMENTS

To the GRÓ GTP Team and the Government of Iceland, thanks for providing the Fellowship, necessary resources and support through this wonderful program that will go a long way in our capacity building, not only as a company but as a country. My personal appreciation to the GRÓ GTP Director Guðni Axelsson for being so flexible with the program, which not only allowed me to pursue the specialization as stipulated but also volunteered to be my main supervisor and arranged for special extra lectures on Reservoir Engineering and Geochemistry of Thermal Fluids.

I want to express my sincere gratitude to my employer, KenGen PLC, for the nomination and time off to undertake this course. Special thanks to the following senior management staff: Mrs. Rebecca Miano (MD and CEO), Eng. Abel Rotich (out-going GDD), Mr. Peketsa Mangi (Ag. GDD) and my line manager, Eng. Peter Ouma. Thanks to all the KenGen Staff who provided me with the data and information whenever I wanted them.

It is a real honour being a student of such accomplished people. I feel indebted to Kjartan, Gunnar, Anette and of course Finnbogi. I would like to sincerely thank them for their assistance and guidance throughout my analysis and compilation of this report. Special thanks to the GRÓ GTP staff led by Ingimar, Vigdís, Frída and Markus (though he left us towards the end of the program) for their generous

help, care, good guidance and advice during my entire study period. I also wish to thank all members of ÍSOR and Orkustofnun who participated in this programme either as lecturers or advisors to make it such a big success. Their doors were always open to us. I appreciate the great input from other organisations and corporations in Iceland. They too supported us fully. To the other GRÓ GTP fellows I say thank you very much for your wonderful company that made me feel at home away from home.

To my beloved wife Jedidah, son Wayne and daughters Precious and Favour, words are not enough to express my sincere gratitude to you for your sacrifice, love and prayers throughout my entire stay in Iceland – may God bless you. Your sacrifice was never in vain.

8. ABBREVIATIONS

AU	Additional Unit
EARS	East African Rift System
GENZL	Geothermal Energy of New Zealand
IRENA	The International Renewable Energy Agency
KenGen	Kenya Electricity Generating Company Limited
KPC	Kenya Power Company Limited
KRS	Kenya Rift System
Ltd	Limited
Masl	Metres above sea level
Mbsl	Metres below sea level
OEPF	Olkaria East Production Field
ONEPF	Olkaria Northeast Production Field
OVC	Olkaria Volcanic Complex
OW	Olkaria Well
PLC	Public Limited Company
PT	Pressure and Temperature

REFERENCES

Adams, M.C., and Davis, J., 1991: Kinetics of fluorescein decay and its application as a geothermal tracer. *Geothermics, 20,* 53-66.

Ambusso, W.J., 1994: Results of injection and tracer tests in Olkaria-East geothermal field. *Proceedings of the 19th Workshop on Geothermal Reservoir Engineering, Stanford University, California*, 155-160.

Ambusso, W.J., and Ouma, P.A., 1991: Thermodynamic and permeability structure of Olkaria North-east geothermal field: Olkaria fault. *Geothermal Resources Council, Transactions, 15,* 237-242.

Arason, Th., Björnsson, G., Axelsson, G., Bjarnason, J.Ö., and Helgason, P., 2004: *ICEBOX – geothermal reservoir engineering software for Windows. A user's manual.* ISOR, Reykjavík, report 2004/014, 80 pp.

Axelsson, G., 2008: The importance of geothermal reinjection. In: Fridleifsson, I.B., Holm, D.H., Wang K., and Zhang B. (eds.), *Workshop for Decision Makers on Direct Heating Use of Geothermal Resources in Asia, Tianjin, China*. UNU-GTP, TBLRREM and TBGMED, CD, 16 pp.

Axelsson, G., 2013a: Tracer tests in geothermal resource management, *EPJ Web of Conferences, 50,* 9 pp.

Axelsson, G., 2013b: Geothermal well testing. *Presented at "Short Course V on Conceptual Modelling of Geothermal Systems"*, *organized by UNU-GTP and LaGeo, Santa Tecla, El Salvador*, 30 pp.

Axelsson, G., 2013c: Dynamic modelling of geothermal systems. *Presented at "SDG Short Course III on Geothermal Reservoir Characterization: Well Logging, Well Testing and Chemical Analysis", organized by UNU-GTP and LaGeo, Santa Tecla, El Salvador*, 21 pp.

Axelsson, G., Björnsson, G., and Montalvo, F., 2005: Quantitative interpretation of tracer test data. *Proceedings of the World Geothermal Congress 2005, Antalya, Turkey*, 12 pp.

Baker, B.H., 1987: Outline of the petrology of the Kenya rift alkaline province. *Geological Society, London, Special Publications, 30(1),* 293-311.

Baker, B.H., Mohr, P.A., and Williams, L.A.J., 1972: Geology of the Eastern Rift System of Africa. *Geol. Soc. of America. Special Paper, 136,* 67 pp.

Bosworth, W., Crevello, P., Winn Jr., R.D. and Steinmetz, J., 1998: Structure, sedimentation, and basin dynamics during rifting of the Gulf of Suez and north-western Red Sea. In: Purser, B.H., and Bosence, D.W.J. (eds.): Sedimentation and tectonics of rift basins: Red Sea - Gulf of Aden. *Chapman and Hall, London*, 77-96.

Bödvarsson, G.S., 1993: *Model for the NE-Olkaria geothermal field*. Kenya Power Company Ltd., internal report.

Bödvarsson, G.S., and Pruess K., 1981: *Olkaria geothermal field numerical studies of the generating capacity of the reservoir.* Kenya Power Company Ltd., internal report.

Bödvarsson, G.S., and Pruess, K., 1984*: History match and performance predictions for the Olkaria geothermal field.* Kenya Power Company Ltd., internal report.

Bunyasi, M.M., 2012: Vulnerability of hydro-electric energy resources in Kenya due to climate change effects: The case of the seven-forks project. *J. Agriculture and Environmental Sciences, 1*, 36-49.

Chorowicz, J., 2005: The East African Rift System. *J. African Earth Sciences*, *43*, 379-410.

Chorowicz, J., Collet, B., Bonavia, F., Mohr, P., Parrot, J.F., and Korme, T., 1998: The Tana basin, Ethiopia: Intra-plateau uplift, rifting and subsidence. *Tectonophysics, 295*, 351–367.

Clarke, M.C.G., Woodhall, D.G., Allen, D., and Darling, G., 1990: *Geological, volcanological and hydrogeological controls of the occurrence of geothermal activity in the area surrounding Lake Naivasha, Kenya*. Report, Ministry of Energy, Kenya.

Diaz, A.R., Kaya, E., Zarrouk, S.J., 2015: Re-injection in geothermal fields - A worldwide review update. *Proceedings World Geothermal Congress 2015, Melbourne, Australia,* 18 pp.

IRENA, 2021: *Renewable capacity statistics 2021*, report, Abu Dhabi, United Arab Emirates, 64 pp. Available at: *www.irena.org/Publications.*

Kagiri, D.N., 1996: Preliminary reinjection trials in the Olkaria northeast field. *Proceedings of 18th NZ Geothermal Workshop,* University of *Auckland*, Geothermal *Institute, New Zealand,* 313-318.

Kamila, Z., Kaya, E., and Zarrouk S.J., 2021. Re-injection in geothermal fields: An updated worldwide

review 2020. *Geothermics, 89,* 101970.

Kandie, R.J., 2017: Borehole geology and thermal history of Well OW-737, Olkaria geothermal field, Kenya. Report 14 in: *Geothermal Training in Iceland 2017*. UNU-GTP, Iceland, 187-220.

Karingithi, C.W., 1993: *Olkaria East production field geochemical report.* Kenya Power Company, Ltd., internal report, 86 pp.

Karingithi, C.W., 1994: *Results of injection and tracer tests in Olkaria Northeast field in Kenya*. Kenya Power Company, internal report.

Karingithi, C.W., 2000: Geochemical characteristics of the Greater Olkaria Geothermal Field, Kenya. Report 9 in: *Geothermal Training in Iceland 2000*. UNU-GTP, Iceland, 165-188.

Kaya, E., Zarrouk, S.J., O'Sullivan, M.J., 2011: Re-injection in geothermal fields: A review of worldwide experience. *Renew. Sustain. Energy Rev., 15,* 47–68.

Koech, V.K., 2014: *Numerical geothermal reservoir modelling and infield re-injection design, constrained by tracer test data: Case study for the Olkaria geothermal field in Kenya.* University of Iceland, MSc thesis, UNU-GTP, report 5, 69 pp.

Koech, V.K., Wafula, E., Githiiyii, S., 2017: *Report for the tracer injection in OW-12*. KenGen PLC, internal report, 27 pp.

KPC, 1981: *Recommendations for further geothermal exploration at Olkaria*. KPC Ltd, internal report.

KPC, 1988. *Proceedings of the scientific review meeting*. KPC Ltd, internal report.

KPLC, 2001: *The Least Cost Power Development Plan: Year 2001 update*. KPLC Ltd, internal report, 114 pp.

Lagat, J.L., 2004: *Geology, hydrothermal alteration and fluid inclusion studies of Olkaria Domes geothermal field, Kenya*. University of Iceland, M.Sc thesis, UNU-GTP, Iceland, report 2, 71 pp.

Lagat, J.L., Arnorsson, S., and Franzson H., 2005. Hydrothermal alteration and fluid inclusion studies of Olkaria Domes geothermal field, Kenya. *Proceedings World Geothermal Congress 2005, Antalya, Turkey,* 14 pp.

Lloyd, P. J., 2017: The role of energy in development. *J. Energy Southern Africa, 28(1),* 54-62.

Mangi, P.M., 2018: Geothermal exploration in Kenya – Status report and updates. *Presented at "SDG Short Course III on Exploration and Development of Geothermal Resources", organized by UNU-GTP and KenGen, at Lake Bogoria and Lake Naivasha, Kenya,* 9-29.

Mariaria, J.M., 2012: Response of Olkaria East Field reservoir to production. *Proceedings, thirty-seventh workshop on Geothermal Reservoir Engineering at Stanford University, Stanford, California,* 7 pp.

Marshall, A.S., Macdonald, R., Rogers, N.W., Fitton, J.G., Tindle, A.G.N., Nejbert, K., and Khinton, R.W., 2009: Fractionation of peralkaline silicic magmas: the Greater Olkaria Volcanic Complex, Kenya Rift valley. *J. Petrol., 50,* 323-359.

Montanari, D., Abanes, R., André L, Asmundson, R., Calore, C.C., Fokker, P., Hopkirk, R.J. Monterrosa, M., Muller, J., Portier, S., Nami, P., Rummel, F., Sanjuan, B., Schindler, M., Seiersten, M.,

Stamatakis, E., Tischner, T., Vuataz, F., and Zimmermann, G., 2008. *Best practice handbook for the development of unconventional geothermal resources with a focus on enhanced geothermal system.* ENGINE Coordination Action, report, 98 pp.

Monterrosa, M.E., and Axelsson, G., 2013: Reservoir response monitoring during production. *Proceedings of the "Short Course on Conceptual Modelling of Geothermal Systems", organized by UNU-GTP and LaGeo, Santa Tecla, El Salvador,* 12 pp.

Muchemi, G.G., 1987. *Geological Report of Well OW-703*. Kenya Power Company, internal report, 31 pp.

Mungania, J., 1992: *Preliminary field report on geology of Olkaria volcanic complex with emphasis on Domes area field investigations*. Kenya Power Company, internal report.

Mungania, J., 1999: *Geological Report of Well OW-714*. Kenya Power Company, internal report.

Munyiri, S., 2016: *Structural mapping of Olkaria Domes geothermal field using geochemical soil gas surveys, remote sensing, and GIS*. University of Iceland, M.Sc thesis, UNU-GTP, Iceland, Report 5, 73 pp.

Mwangi, M.N., 2000: Country initial update report for Kenya 1995 - 1999. *Proceedings of World geothermal congress 2000, Kyushu-Tohoku, Japan,* 327-335.

Mwania, M., Munyiri, S., and Okech, E., 2013: *Borehole geology and hydrothermal mineralisation of Well OW-35, Olkaria East geothermal field, Central Kenya Rift Valley.* UNU-GTP, Iceland, report 1, 56 pp.

Mwawongo, G.M., 2004: Infield re-injection strategies in Olkaria, Kenya, based on tracer studies and numerical modelling. Report 12 in: *Geothermal Training in Iceland 2004*. UNU-GTP, Iceland, 239-266.

Naylor, W.I., 1972: *Geology of the Eburru and Olkaria prospects*. UN Geothermal Exploration Project report, 104 pp.

Ofwona, C.O., 1996: Analysis of injection and tracer tests data from the Olkaria East geothermal field Kenya. Report 10 in: *Geothermal Training in Iceland 1996*. UNU-GTP, Iceland, 197-218.

Ofwona, C.O., 2002: *A reservoir study of Olkaria East geothermal system, Kenya*. University of Iceland, M.Sc. thesis, UNU-GTP, Iceland, report 1, 74 pp.

Ofwona, C.O., 2010: Olkaria I reservoir response to 28 years of production. *Proceedings of the World Geothermal Congress 2010, Bali, Indonesia,* 4 pp.

Ofwona, C.O., 2005: Olkaria reservoir response to exploitation and future development. Lecture 3 in: Mwangi, M. (lecturer), *Lectures on the geothermal in Kenya and Africa*. UNU-GTP, Iceland, Report 4, 29-40.

Ogoso-Odongo, M.E., 1986: Geology of the Olkaria geothermal field. *Geothermics, 15*, 741-748.

Ojiambo, B.S., and Lyons, W.B., 1993: Stable isotope composition of Olkaria geothermal field fluids, Kenya. *Geothermal Resources Council Transactions, 17,* 149-154.

Okoo, J., Omiti, A., Kimunya K., and Saitet, D., 2017: Updated conceptual model of Olkaria geothermal field Naivasha, Kenya. *Geothermal Resources Council Transactions, 41*, 18 pp.

Omenda, P.A., 1994: The geological structure of the Olkaria west geothermal field, Kenya. *Proceedings of the 19th Stanford Geothermal Reservoir Engineering Workshop, Stanford, CA,* 125-130.

Omenda, P.A, 1998: The geology and structural controls of the Olkaria geothermal system, Kenya. *Geothermics, 27(1),* 55-74.

Omenda, P.A., 2000: Anatectic origin for comendite in Olkaria geothermal field, Kenya Rift; geochemical evidence for syenitic protholith. *African Journal of Science and Technology, 1,* 39-47.

Otieno, V.O., 2016: *Borehole geology and sub-surface petrochemistry of the Domes area, Olkaria geothermal field, Kenya, in relation to well OW-922*. University of Iceland, M.Sc thesis, UNU-GTP, Iceland, 114 pp.

Ouma, P.A., 1992: *Steam gathering system for the NE-Olkaria geothermal field, Kenya – preliminary design*. UNU-GTP, Iceland, report 9, 47 pp.

Ouma, P.A., 2005: Reservoir engineering and geothermal power production in Olkaria. *Paper presented at "Workshop for Decision Makers on Geothermal Projects and Management", organized by UNU-GTP and KenGen in Naivasha, Kenya,* 12 pp.

Ouma, P.A, 2009: Geothermal exploration and development of the Olkaria geothermal field. *Presented at "Short Course IV on Exploration for Geothermal Resources", organized by UNU-GTP, KenGen and GDC, at Lake Naivasha, Kenya,* 16 pp.

Roberts, E., Stevens, N., O'Connor, P., Dirks, P., Gottfried, M., Clyde, W., Armstrong, R., Kemp. A.I.S., and Hemming, S., 2012: Initiation of the western branch of the East African Rift coeval with the eastern branch. *Nature Geoscience, 5,* 289-294.

Rose, P., Benoir, D., Lee, S.G., Tandia, B., and Kilbourn, P., 2000: Testing the naphthalene sulfonates as geothermal tracers at Dixie Valley, Ohaki and Awibengkok. *Proceedings of the 25th Workshop on Geothermal Reservoir Engineering, Stanford University, Stanford, CA.,* 7 pp.

Saemundsson, K., 2010: East African Rift System - An Overview. *Presented at "Short Course V on Exploration for Geothermal Resources", organized by UNU-GTP, GDC and KenGen, at Lake Bogoria and Lake Naivasha, Kenya,* 8 pp.

Sverrisdóttir, S.B., 2016: *Tracer testing in the Svartsengi geothermal field in 2015*. Reykjavik University, M.Sc thesis, Iceland, 85 pp.

Smith, M. and Mosley, P., 1993: Crustal heterogeneity and basement influence on the development of the Kenya rift, East Africa. *Tectonics, 12*, 591-606.

Wamalwa, R.N., Nyamai, C.M., Ambusso, W.J., Mulwa, J., and Waswa, A.K, 2016: Structural controls on the geochemistry and output of the wells in the Olkaria geothermal field of the Kenyan Rift Valley. *International Journal of Geosciences, 7(11),* 1299-1309.

Wamalwa, R.N., and Nyawir, E.O., 2020a: *Report for the tracer injection in OW-34*. KenGen PLC, internal report, 19 pp.

Wamalwa, R.N., and Nyawir, E.O., 2020b: *Report for the tracer injection in OW-928*. KenGen PLC, internal report, 37 pp.